

Research paper

Bayesian Interactive Search Algorithm: A New Probabilistic Swarm Intelligence Tested on Mathematical and Structural Optimization Problems

Ali Mortazavi

Graduate School of Natural and Applied Sciences, Ege University, Izmir, Turkey

ARTICLE INFO

Keywords:

Metaheuristic algorithms
Bayesian approach
Structural and mathematical optimization problems

ABSTRACT

Metaheuristic algorithms are general optimization techniques that demonstrate remarkable performance in solving different classes of optimization problems. However, equipping their stochastic search mechanisms with auxiliary logical strategies can still increase their search capability. Based on this fact, in the current study, the search performance of the Interactive Search Algorithm (ISA), as a metaheuristic search method, is improved by adding a new Bayesian regulator strategy to adjust its search behavior. In this regard, the search patterns of the ISA method are unified and classified according to the memory and learning concepts. Subsequently, during the optimization process, the developed Bayesian module dynamically regulates the ratio of the exploration and exploitation search behaviors by tuning the effect of memory concept. The recent technique is named Bayesian Interactive Search Algorithm (BISA), and its search performance tested on a suite of unconstrained mathematical functions and constrained engineering problems. Acquired outcomes indicate that the proposed BISA considerably speeds up the convergence rate, and improves the stability of the process as well as the accuracy of the solutions, for both engineering and mathematical problems.

1. Introduction

Generally, the metaheuristic algorithms are population-based and gradient-free search techniques inspired by the natural rules or physical and/or social phenomena [1-5]. They do not demand any continuous objective function and its gradient information to determine the search direction and step sizes. This feature makes them convenient techniques to solve complex optimization problems in which it is very difficult (or even impossible) to define the continuous and differentiable objective functions. On this subject, in the last decades, these methods are broadly employed to solve different mathematical and engineering optimization problems [6-18].

Based on the existing studies, although each of these methods has its weaknesses and strengths in solving different problems, they are mostly suffered from the lack of a proper trade-off between exploration and exploitation balance specially in the case of more complicated optimization problems. To mitigate this shortcoming, there are several works addressed in the literature [19-26]. Some of them hybridize the affirmative local and global search capabilities of two or more methods, while some other add the auxiliary module(s) to the algorithm to tune its search behavior. As the instances, Wen-Jun and Xiao-Feng (2003) combined Differential Evolution (DE) with Particle Swarm Optimization

(PSO) [27], Deep et al. (2009) hybridized Genetic Algorithm (GA) and PSO with Quadratic Approximation (QA) [28,29], Barroso et al. (2017) proposed a hybrid GA-PSO to optimize the laminated composites [30]. Yalaoui et al. (2013) applied a fuzzy programming in solving scheduling problem [31]; Nobile et al. (2018) introduced a fuzzy formulation for adjusting the search behavior of PSO algorithm [32]. To provide a deeper insight into the previous studies, Table 1 chronologically summarizes some relevant work done in the last decade.

Interactive Search Algorithm (ISA) is one of these methods which is the recently developed. It employs a search strategy consists of two distinct search patterns called *tracking* and *interacting* phases. The proposed ISA applies *tendency factor* as an internal parameter to adjust the balance between these two phases. This algorithm shows a good performance on solving mathematical and structural problems [41,44]. However, assessing the work mechanism of ISA reveals that it still has two drawbacks. First, to increase the search capacity of this method, its internal setting parameter (i.e. tendency factor) should be determined for the current optimization problem performing a series of costly sensitivity analyses. Second, in the interacting phase of the algorithm a simple random search direction is provided which cannot accomplish the required local search particularly in the case of complex optimization problems.

E-mail address: ali.mortazavi.phd@gmail.com.

<https://doi.org/10.1016/j.advengsoft.2021.102994>

Received 20 October 2020; Received in revised form 9 January 2021; Accepted 3 March 2021

Available online 19 March 2021

0965-9978/© 2021 Elsevier Ltd. All rights reserved.

Table 1
Literature review of improvements of metaheuristic methods.

No.	Year	Author	Ref.	Inspiration/Innovation
1	2010	Xin et al.	[33]	Hybridizing DE ^{*1} and PSO ^{*2} methods
2	2012	Deng et al.	[34]	Hybridizing PSO, ACO ^{*3} and GA ^{*4}
3	2013	Finotto et al.	[35]	Using the Fuzzy Logic to adjust GA
4	2015	Olivas et al.	[36]	Applying the Fuzzy Logic for adjusting ACO
5	2016	Mlakar et al.	[20]	Introducing hybrid self-adaptive CS ^{*5} algorithm using linear population reduction
6	2016	Mortazavi et al.	[37]	Introducing Improved Fly-back approach to improve handling of constraints
7	2017	Kumar et al.	[38]	Improving the local search of BO ^{*6} using Covariance Matrix
8	2017	Barroso et al.	[30]	Combining GA and PSO
9	2018	Lieu et al.	[39]	Introducing an adaptive hybrid evolutionary firefly algorithm
10	2018	Mortazavi et al.	[40]	Integrating learning mechanism to improve exploitation behavior of iPSO ^{*7}
11	2018	Nobile et al.	[41]	Introducing Fuzzy mechanism to adjust PSO method
12	2019	Le et al.	[42]	Combining firefly algorithms and electromagnetism-like mechanism
13	2019	Sun et al.	[43]	Applying opposition-based learning to improve exploration of MBO ^{*8} method

*1 Deferential Evolution (DE) optimization

*2 Particle Swarm Optimization (PSO)

*3 Ant Colony Optimization (ACO)

*4 Genetic Algorithm

*5 Cuckoo Search

*6 Butterfly Optimization Algorithm

*7 Ingrated PSO

*8 Monarch Butterfly Optimization

In the current study, initially the search patterns of the ISA algorithm (i.e. tracking and interacting) are combined together. Then, the components of the unified formulation are divided into memory and learning concepts. Consequently, a Bayesian regulator formulation is developed to tuned the contribution level of the memory concept in the search process. Such that, increasing and decreasing the impact of the memory concept respectively amplifies the exploration and exploitation search behaviors of the algorithm. The recent method is named Bayesian Interactive Search Algorithm (BISA). Bayesian regulating mechanism of the proposed BISA provides two main advantages in comparison with conventional approaches (e.g. fuzzy-based mechanisms). First, it is based on probabilistic rules and its developing/application does not require any prior user knowledge about the problem and/or the how the search algorithm works. Second, it dynamically adjusts the algorithm search behavior based on the governing conditions of the current problem, therefore it gives a self-adaptive property to the algorithm. Consequently, the search performance of the proposed BISA is tested on a suite of different constrained and unconstrained optimization problems with both continuous and discrete variables and the acquired results are reported and discussed.

The rest of this study is organized as follows. In the next section, ISA method is briefly described. In section 3, the proposed BISA and its Bayesian decision mechanism are described in detail. The Section 4 is devoted to test the search performance of proposed BISA on distinct mathematical and engineering optimization problems. In section 5, to

give more insight about introduced method, its important features are discussed in more detail. Consequently, a brief conclusion on achievements and observations is given in the last section.

2. Interactive Search Algorithm (ISA)

In the current section, Interactive Search Algorithm (ISA) is concisely described. The ISA method is the gradient-free and population-based search algorithm which has been introduced by Mortazavi et al. [40]. Each agent in the ISA method, based on its tendency factor (τ_i) uses either tracking or interacting phase to update its location. In the tracking phase, the agent searches the vicinity of the locations spotted three certain agents as the best agent (X^G), the weighted agent (X^W), and best location of a random agent saved in the prior best matrix (X^P). In the interacting phase, the agent updates its location based on a pairwise knowledge sharing with other random agent. The ISA method is mathematically formulated as follows:

if $\tau_i \geq 0.3$ [Tracking phase] :

$${}^{t+1}V_i = \omega_0 \cdot {}^tV_i + \phi_1 ({}^tX_i^P - {}^tX_i) + \phi_2 ({}^tX^G - {}^tX_i) + \phi_3 ({}^tX^W - {}^tX_i) \quad (1.1)$$

if $\tau_i < 0.3$ [Interacting phase] :

$${}^{t+1}V_i = \phi_4 ({}^tX_j - {}^tX_i) \quad (1.2)$$

Updating formulation :

$${}^{t+1}X_i = {}^tX_i + {}^{t+1}V_i \quad (1.3)$$

in which, the upper left superscripts “t+1” and “t” indicate the updated and current states of the variables, respectively; τ_i is the tendency factor randomly selected from the [0,1] interval; ω_0 is the coefficient which is constantly taken as 0.4 [37,40]. ϕ_1, ϕ_2 and ϕ_3 are the coefficients of acceleration and picked randomly from the [0, 1] interval; ${}^tX^P$, tX , and ${}^tX^G$ are respectively the agent randomly selected from the agents' saved previous best locations, the current agent, and the best agent. Also, X^W is the weighted agent defined as the weighted average of all population and mathematically formulated as below [40].

$$X^W = \sum_{i=1}^{PS} \bar{c}_i^w X_i^P$$

where,

$$\bar{c}_i^w = \left(\hat{c}_i^w / \sum_{i=1}^{PS} \hat{c}_i^w \right) \quad (2)$$

and

$$\hat{c}_i^w = \frac{\max_{1 \leq k \leq PS} (f(X_k^P)) - f(X_i^P)}{\max_{1 \leq k \leq PS} (f(X_k^P)) - \min_{1 \leq k \leq PS} (f(X_k^P)) + \mu}, \quad i = 1, 2, \dots, PS$$

in this formulation, PS represents the population size and $f(\cdot)$ returns the objective function value for selected agent. Also, μ is a small positive number to avoid probable division by zero conditions and taken as 1E-5. In the next section the proposed new method is given in detail.

3. Bayesian Interactive Search Algorithm (BISA)

Based on the given definitions in the previous section, in the ISA approach the tendency factor reveals that, the interacting search phase

Table 2
The illustrations of the term used by BISA updating formulation.

Term	Work Mechanism	Classified Concept	
$\omega \cdot V$	Remembering and implementing the previous search direction	Memory	Memory
$\varphi_1 \odot ({}^t X_i^P - {}^t X_i)$	Learning from its earned individual experiences (${}^t X_i^P$)	Individual Learning	Learning
$\varphi_2 \odot ({}^t X^G - {}^t X_i^P)$	Learning from the best agent of the population (${}^t X^G$)	General Learning	
$\varphi_3 \odot ({}^t X^W - {}^t X_i)$	Learning from the weighted average of the population (${}^t X^W$)	Elitism Learning	
$\varphi_4 \odot ({}^t X^J - {}^t X_i)$	Learning from the random agent of the population (${}^t X^J$)	Pairwise Learning	

accounts thirty percent of the search capacity of the ISA method. However, studies show that in the more complex problems decreasing the contribution of this phase does not considerably affects the search performance of the method [45,46]. Also, the ISA applies a simple random approach to adjust its search behavior that does not take into account the governing conditions of the current problem. Therefore, to overcome these two shortcomings and provide a single-phase and self-adaptive search algorithm, in the current section, initially, both the tracking and interacting phases of the ISA method are combined as given

$$\begin{aligned}
 {}^{t+1}X - {}^tX &= \omega({}^tX - {}^{t-1}X) + \varphi_1(X^P - {}^tX) + \varphi_2(X^G - {}^tX) + \varphi_3(X^W - {}^tX) + \varphi_4({}^tX_j - {}^tX) \\
 &\text{so,} \\
 {}^{t+1}X &= {}^tX + \omega({}^tX - {}^{t-1}X) + \varphi_1 X^P - \varphi_1 {}^tX + \varphi_2 X^G - \varphi_2 {}^tX + \varphi_3 X^W - \varphi_3 {}^tX + \varphi_4 X^j - \varphi_4 {}^tX \\
 &\text{by factorization and simplification,} \\
 {}^{t+1}X &= (1 + \omega) {}^tX - \omega {}^{t-1}X + \Psi \\
 &\text{where,} \\
 \Psi &= (\varphi_1 X^P + \varphi_2 X^G + \varphi_3 X^W + \varphi_4 X^j) - (\varphi_1 + \varphi_2 + \varphi_3 + \varphi_4) {}^tX
 \end{aligned} \tag{5}$$

in Eq. (3). Later, the resulting hybrid formulation is rearranged based on the *memory* and *learning* concepts. Finally, it is equipped with a Bayesian decision-making formulation to adjust the search behavior of the algorithm by dynamically regulating the impact of the memory concept on the navigation process. The new algorithm is named Bayesian Interactive Search Algorithm (BISA) and its updating process is formulated as follows:

$$\begin{aligned}
 {}^{t+1}V_i &= \omega \cdot V + \varphi_1 ({}^t X_i^P - {}^t X_i) + \varphi_2 ({}^t X^G - {}^t X_i) + \varphi_3 ({}^t X^W - {}^t X_i) + \varphi_4 ({}^t X^j - {}^t X_i) \\
 \text{Updating formulation:} \\
 {}^{t+1}X_i &= {}^t X_i + {}^{t+1}V_i
 \end{aligned} \tag{3}$$

The definitions for each term is the same as given in previous section for ISA method, just the ω_0 is replace by ω for simplicity. To make a deeper insight into given formulation, its components are classified based on the *memory* and *learning* concepts. Table 2 gives details about this classification.

According to the given definitions, the proposed BISA in the learning mode, generally searches the vicinity of some other promising agents. This means that the learning process mostly provides an exploitation search behavior of the algorithm especially in the further iterations that agents mostly stand close to each other due to dropping of the population diversity [40]. However, the memory concept generating an alternative search direction increases the randomness of the search process and emphasizes the exploration search behavior of the algorithm [47]. On the other words, by increasing the contribution of the memory concept, the exploration search behavior is considerably intensified, while eliminating the role of the memory concept, puts the algorithm in

the pure exploitation search mode. This fact is proven and shown for PSO (and PSO-based) algorithms in several studies [48,49]. Subsequently, since the BISA is also belongs to this class of optimization methods (with extended learning patterns), its search behavior follows the same logic. Using this fact, to provide a self-adaptive search algorithm, in the next section a hierarchical Bayesian approach is applied for dynamically adjusting the contribution rate of the memory concept in the navigation process of BISA.

3.1. Bayesian Regulator Formulation for BISA

In the proposed BISA, the participation rate of the memory concept is controlled by ω factor (see Eq. (3)), since from now on, it is named as *memory impact factor*. To adjust the contribution rate of the memory concept, the memory impact factor (ω) is taken as the adjustable parameter for the proposed Bayesian process. For implementing the Bayesian approach Eq. (3) is re-written as below:

$$\begin{aligned}
 {}^{t+1}X &= {}^tX + {}^{t+1}V \\
 \text{so,} \\
 {}^{t+1}V &= {}^{t+1}X - {}^tX \text{ and } {}^tV = {}^tX - {}^{t-1}X
 \end{aligned} \tag{4}$$

By substituting,

In the given formulations, the left superscripts $t+1$, t , and $t-1$, denote the updated, current and previous conditions of the corresponding variable, respectively. Considering $W_1 = (1 + \omega)$ and $W_2 = -\omega$ and putting the variables in the corresponding vectors, it is obtained as: ${}^tW = [W_1, W_2]^T$, ${}^t\Omega = [{}^tX, {}^{t-1}X]^T$, so for k th iteration $\Omega = [{}^t\Omega, {}^{t+1}\Omega, \dots, {}^{t+k-1}\Omega]^T$ and $Q = [{}^{t+1}X, {}^{t+2}X, \dots, {}^{t+k}X]^T$. Consequently, the generalized updating formulation for k th iteration can be written as below:

$$Q = \Omega W + \Psi \tag{6}$$

Since the multivariate Gaussian distribution is well-fitted with the most of the probabilistic problems, it is implemented for the probabilistic model, so the normal distribution for proposed W parameter is formulated as below:

$$\begin{aligned}
 P(W) &= \frac{1}{Z_W(\alpha)} \exp(-\alpha E_W) \\
 E_W &= \frac{1}{2} \|W\|^2 = \sum_{i=1}^M (W_i)^2
 \end{aligned} \tag{7}$$

in which, α is the distribution control parameter and $\|\bullet\|$ returns the second norm of the desired vector. Also, $P(W)$ is the normal probability distribution of W , and M denotes the number of contributed elements. Normalization factor for given distribution is shown by $Z_W(\alpha)$ and it is obtained as:

$$Z_W(\alpha) = \int \exp(-\alpha E_W) = \left(\frac{2\pi}{\alpha}\right)^{\frac{M}{2}} \tag{8}$$

The likelihood for the problem is calculated as follows:

$$P(D|W) = \frac{1}{Z_D(\beta)} \exp(-\beta E_D) \tag{9}$$

in which, E_D denotes the error function, and β is the distribution controller factor. Also, $Z_D(\beta)$ is the normalization factor of the distribution. Considering that D is selected as the general abbreviation for data, the formulation is expanded as below:

$$P(D|W) = P(Q|(W, \Omega)) = \prod_{i=1}^k P({}^{t+i}X|(W, \Omega)) = \frac{1}{Z_D(\beta)} \exp\left(-\frac{\beta}{2} \sum_{i=1}^k ({}^{t+i}X - \Omega_i W)^2\right) \tag{10}$$

where,

$$Z_D(\beta) = \int \exp(-\beta E_D) = \left(\frac{2\pi}{\beta}\right)^{\frac{k}{2}}$$

Defining likelihood and prior distributions the posterior distribution over the memory impact factor's space is attained as follows:

$$P(W|D) = \frac{P(D|W) P(W)}{P(D)} \tag{11}$$

Substituting Eqs. (7) and (9) into Eq. (11) the posterior distribution is obtained as follows:

$$P(W|D) = \frac{1}{Z_S} \exp(-\alpha E_W - \beta E_D) = \frac{1}{Z_S} \exp(-S(W)) \tag{12}$$

where

$$S(W) = \alpha E_W + \beta E_D$$

$$Z_S(\alpha, \beta) = \int \exp(-S(W)) = \int \exp(-(\alpha E_W + \beta E_D)) dW$$

Based on the hierarchical Bayesian approach the hyperparameters of the problem should be declared before maximizing the posterior of the problem. This process is given in the next sub-section.

3.1.1. Determination of Hyperparameters α and β

In this section the controller parameter (α, β) are determined as the

Table 3

The pseudo code for the BISA

```

Generate random population of agents
Randomly initiate the memory impact factors( $\omega$ ) for agents
while (termination conditions are not met)
Set the best agent of the population as ( $X^G$ )
Calculate the weighted agent ( $X^W$  for the current population using Eq. (2)
for (each particle i)
Record Bayesian information**
if activation period of the Bayesian module is reached [mod(i/k) = 0]**
Adjust the memory impact factor using Eq. (22)
end
Update current agent using Eq. (3)
if updated agent is better than the current agent
Hold updated agent and replace the current agent
else
Reject updated agent and hold the current agent
end
end
end
end
    
```

* : For the minimization problem, X^G is the agent with the lowest objective function value.

** : Required procedure to gather the Bayesian information e.g. evidence and data (Q, Ω) is described in detail in sub-section 3.1.

*** : Based on analyses performed in section 5, $k=10$ is recommended.

part of the hierarchical Bayesian approach. In this regard, the posterior distribution can be expanded base on the hyperparameters (α, β) as:

$$P(W|D) = \int \int P(W, \alpha, \beta|D) d\alpha d\beta \tag{13}$$

$$= \int \int P(W|\alpha, \beta, D) P(\alpha, \beta|D) d\alpha d\beta$$

To simplify the solution, it is assumed that $P(\alpha, \beta|D)$ is sharply peaked around the most probable values of α_{MP}, β_{MP} , so the posterior can be re-written as below:

$$P(W|D) = P(W|\alpha_{MP}, \beta_{MP}, D) \int \int P(\alpha, \beta|D) d\alpha d\beta \tag{14}$$

$$= P(W|\alpha_{MP}, \beta_{MP}, D)$$

Base on the applied hierarchical Bayesian approach, in order to determine the α_{MP}, β_{MP} the posterior distribution for of hyperparameter should be evaluated as follow:

$$P(\alpha, \beta|D) = \frac{P(D|\alpha, \beta) P(\alpha, \beta)}{P(D)} \tag{15}$$

Considering the dependencies of α, β explicitly the evidence distribution can be written as follows:

$$P(D|\alpha, \beta) = \int P(D|W, \alpha, \beta) P(W|\alpha, \beta) dW \tag{16}$$

$$= \int P(D|W, \beta) P(W|\alpha) dW$$

Combining Eqs. (7) and (12) into Eq. (16) the dominator term can be rewritten as:

$$P(D|\alpha, \beta) = \frac{1}{Z_D(\beta)} \frac{1}{Z_W(\alpha)} \int \exp(-S(W)) dW = \frac{Z_S(\alpha, \beta)}{Z_D(\beta) Z_W(\alpha)} \tag{17}$$

The logarithmic form of evidence is written as follows:

$$\ln P(D|\alpha, \beta) = -\alpha E_W^{MP} - \beta E_D^{MP} - \frac{1}{2} \ln|A| + \frac{M}{2} \ln \alpha + \frac{K}{2} \ln \beta - \frac{K}{2} \ln(2\pi) \tag{18}$$

The optimal hyperparameters are obtained after differentiating Eq. (18) as follows [50]:

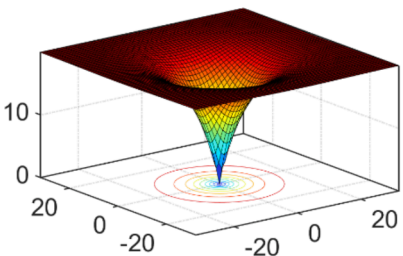
Table 4

Parameter setting for the applied algorithms.

*Algorithm	Year	Parameter
FA [51]	2009	$\alpha = 0.5, \beta_{min} = 0.2, \gamma = 1$
TLBO [52]	2011	$TF = \text{round}[1 + \text{rand}(0, 1)\{2 - 1\}]$
DSO [53]	2014	-
iPSO [54]	2017	$\alpha = 0.4, C_3 = C_4 = 1, C_2 = 2$
ISA [14]	2019	$\tau = 0.3, \omega = 0.4$
BISA	Current Study	-

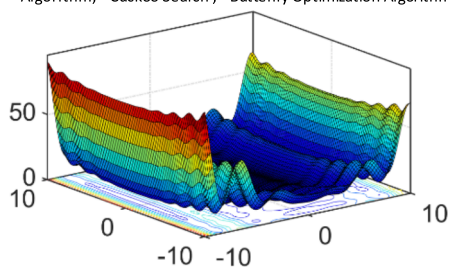
* FA: Firefly Algorithm; TLBO: Teaching and learning Based Optimization; DSO: Drosophila food-Search Algorithm; iPSO: integrated Particle Swarm Optimization; ISA: Interactive Search Algorithm; BISA: Bayesian Interactive Search Algorithm

Table 5
Benchmark functions and their properties.

Function	Properties	Schematic Plot	Formulation**	min																																																																						
F1: Ackley	-UM* -NS*	<table border="1"> <thead> <tr> <th>No.</th> <th>Year</th> <th>Author</th> <th>Ref.</th> <th>Inspiration/Innovation</th> </tr> </thead> <tbody> <tr> <td>1</td> <td>2010</td> <td>Xin et al.</td> <td>[33]</td> <td>Hybridizing DE^{*1} and PSO^{*2} methods</td> </tr> <tr> <td>2</td> <td>2012</td> <td>Deng et al.</td> <td>[34]</td> <td>Hybridizing PSO, ACO^{*3} and GA^{*4}</td> </tr> <tr> <td>3</td> <td>2013</td> <td>Finotto et al.</td> <td>[35]</td> <td>Using the Fuzzy Logic to adjust GA</td> </tr> <tr> <td>4</td> <td>2015</td> <td>Olivas et al.</td> <td>[36]</td> <td>Applying the Fuzzy Logic for adjusting ACO</td> </tr> <tr> <td>5</td> <td>2016</td> <td>Mlakar et al.</td> <td>[20]</td> <td>Introducing hybrid self-adaptive CS^{*5} algorithm using linear population reduction</td> </tr> <tr> <td>6</td> <td>2016</td> <td>Mortazavi et al.</td> <td>[37]</td> <td>Introducing Improved Fly-back approach to improve handling of constraints</td> </tr> <tr> <td>7</td> <td>2017</td> <td>Kumar et al.</td> <td>[38]</td> <td>Improving the local search of BO^{*6} using Covariance Matrix</td> </tr> <tr> <td>8</td> <td>2017</td> <td>Barroso et al.</td> <td>[30]</td> <td>Combining GA and PSO</td> </tr> <tr> <td>9</td> <td>2018</td> <td>Lieu et al.</td> <td>[39]</td> <td>Introducing an adaptive hybrid evolutionary firefly algorithm</td> </tr> <tr> <td>10</td> <td>2018</td> <td>Mortazavi et al.</td> <td>[40]</td> <td>Integrating learning mechanism to improve exploitation behavior of iPSO^{*7}</td> </tr> <tr> <td>11</td> <td>2018</td> <td>Nobile et al.</td> <td>[41]</td> <td>Introducing Fuzzy mechanism to adjust PSO method</td> </tr> <tr> <td>12</td> <td>2019</td> <td>Le et al.</td> <td>[42]</td> <td>Combining firefly algorithms and electromagnetism-like mechanism</td> </tr> <tr> <td>13</td> <td>2019</td> <td>Sun et al.</td> <td>[43]</td> <td>Applying opposition-based learning to improve exploration of MBO^{*8} method</td> </tr> </tbody> </table>	No.	Year	Author	Ref.	Inspiration/Innovation	1	2010	Xin et al.	[33]	Hybridizing DE ^{*1} and PSO ^{*2} methods	2	2012	Deng et al.	[34]	Hybridizing PSO, ACO ^{*3} and GA ^{*4}	3	2013	Finotto et al.	[35]	Using the Fuzzy Logic to adjust GA	4	2015	Olivas et al.	[36]	Applying the Fuzzy Logic for adjusting ACO	5	2016	Mlakar et al.	[20]	Introducing hybrid self-adaptive CS ^{*5} algorithm using linear population reduction	6	2016	Mortazavi et al.	[37]	Introducing Improved Fly-back approach to improve handling of constraints	7	2017	Kumar et al.	[38]	Improving the local search of BO ^{*6} using Covariance Matrix	8	2017	Barroso et al.	[30]	Combining GA and PSO	9	2018	Lieu et al.	[39]	Introducing an adaptive hybrid evolutionary firefly algorithm	10	2018	Mortazavi et al.	[40]	Integrating learning mechanism to improve exploitation behavior of iPSO ^{*7}	11	2018	Nobile et al.	[41]	Introducing Fuzzy mechanism to adjust PSO method	12	2019	Le et al.	[42]	Combining firefly algorithms and electromagnetism-like mechanism	13	2019	Sun et al.	[43]	Applying opposition-based learning to improve exploration of MBO ^{*8} method	$f(\mathbf{X}) = -20 \exp \left(-0.2 \sqrt{\frac{1}{D} \sum_{i=1}^D x_i^2} \right) - \exp \left(\sum_{i=1}^D \cos \left(\frac{2\pi x_i}{D} \right) + 20 + e \right)$	0
No.	Year	Author	Ref.	Inspiration/Innovation																																																																						
1	2010	Xin et al.	[33]	Hybridizing DE ^{*1} and PSO ^{*2} methods																																																																						
2	2012	Deng et al.	[34]	Hybridizing PSO, ACO ^{*3} and GA ^{*4}																																																																						
3	2013	Finotto et al.	[35]	Using the Fuzzy Logic to adjust GA																																																																						
4	2015	Olivas et al.	[36]	Applying the Fuzzy Logic for adjusting ACO																																																																						
5	2016	Mlakar et al.	[20]	Introducing hybrid self-adaptive CS ^{*5} algorithm using linear population reduction																																																																						
6	2016	Mortazavi et al.	[37]	Introducing Improved Fly-back approach to improve handling of constraints																																																																						
7	2017	Kumar et al.	[38]	Improving the local search of BO ^{*6} using Covariance Matrix																																																																						
8	2017	Barroso et al.	[30]	Combining GA and PSO																																																																						
9	2018	Lieu et al.	[39]	Introducing an adaptive hybrid evolutionary firefly algorithm																																																																						
10	2018	Mortazavi et al.	[40]	Integrating learning mechanism to improve exploitation behavior of iPSO ^{*7}																																																																						
11	2018	Nobile et al.	[41]	Introducing Fuzzy mechanism to adjust PSO method																																																																						
12	2019	Le et al.	[42]	Combining firefly algorithms and electromagnetism-like mechanism																																																																						
13	2019	Sun et al.	[43]	Applying opposition-based learning to improve exploration of MBO ^{*8} method																																																																						
																																																																										

*1 Deferential Evolution (DE) optimization, *2 Particle Swarm Optimization (PSO), *3 Ant Colony Optimization (ACO), *4 Genetic Algorithm, *5 Cuckoo Search, *6 Butterfly Optimization Algorithm, *7 Ingrated PSO, *8 Monarch Butterfly Optimization

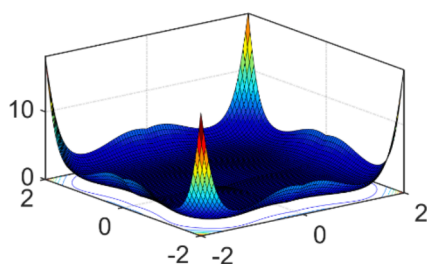
F2: Levy
-UM*
-NS*
-SC*



$$f(\mathbf{X}) = \sin^2(\pi w_1) + \sum_{i=1}^{D-1} (w_i - 1)^2 [1 + 10 \sin^2(\pi w_1 + 1)] + (w_D - 1)^2 [1 + \sin^2(2\pi w_D)]$$

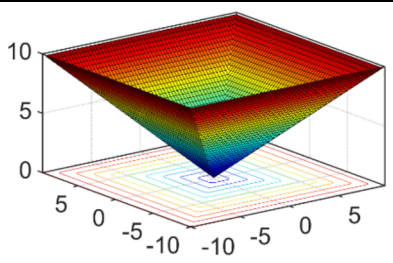
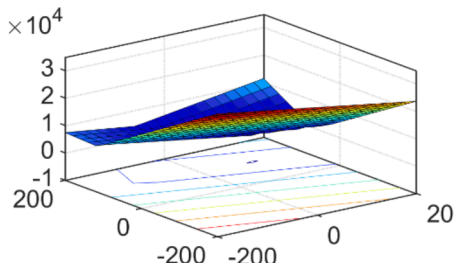
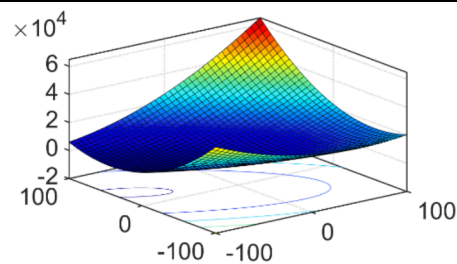
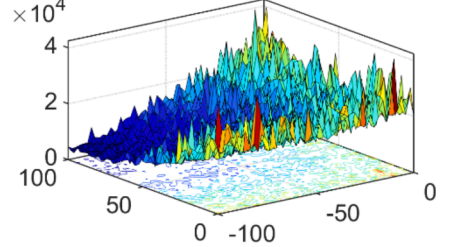
$$w_i = 1 + \frac{x_i - 1}{4}$$

F3: Xin-She Yang N. 2
-MM*
-NS*
-A*
-LOH*



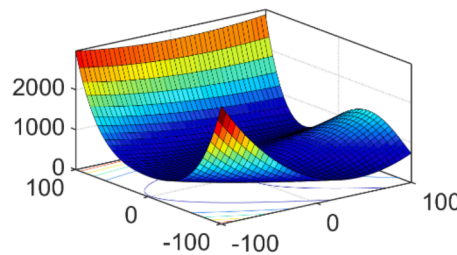
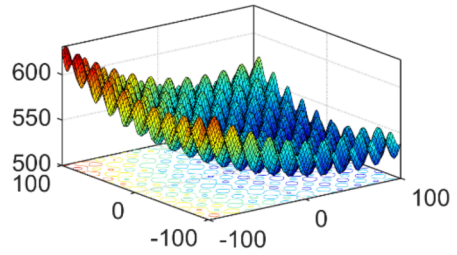
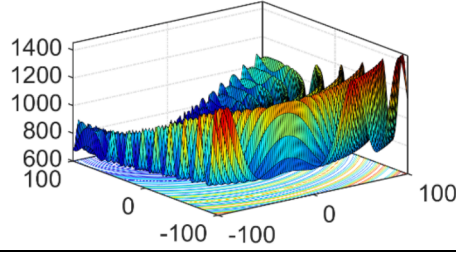
$$f(\mathbf{X}) = \left(\sum_{i=1}^D |x_i| \right) \exp \left(- \sum_{i=1}^D \sin(x_i^2) \right)$$

Table 5 (continued)

Function	Properties	Schematic Plot	Formulation**	min
F4: Schwefel 2.21	-UM* -NS*		$f(\mathbf{X}) = \max_{i=1, \dots, D} x_i $	0
F5: Schwefel's Problem 2.6 with Global Optimum on Bounds	-UM* -NS* -S* -R*		$f(\mathbf{X}) = \sum_{i=1}^D (10^6)^{\frac{i-1}{D-1}} z_i^2 - 450 z = (x - o)M, \mathbf{X} = [x_1, x_2, \dots, x_D]$	-450
F6: Shifted Rotated High Conditioned Elliptic Function	-UM* -NS* -S* -SC*		$f(\mathbf{X}) = \sum_{i=1}^D (10^6)^{\frac{i-1}{D-1}} z_i^2 - 450$	-450
F7: Shifted Schwefel's Problem 1.2 with Noise in Fitness	-MM* -S* -NS* -SC*		$f(\mathbf{X}) = (\sum_{i=1}^D (\sum_{j=1}^i z_j))^2 * (1 + 0.4N(0,1)) - 450$	-450

(continued on next page)

Table 5 (continued)

Function	Properties	Schematic Plot	Formulation**	min
F8: Shifted and Rotated Rosenbrock	-MM* -NS* -LOH*		$L(\mathbf{X}) = \sum_{i=1}^{D-1} (100(x_i^2 - x_{i+1})^2 + (x_i - 1)^2) f(\mathbf{X}) = L\left(M\left(\frac{2.048(x - o)}{100}\right) + 1\right) + 400$	400
F9: Shifted and Rotated Rastrigin	-MM* -NS* -LOH*		$L(\mathbf{X}) = \sum_{i=1}^D (x_i^2 - 10\cos(2\pi x_i) + 10) f(\mathbf{X}) = L(M(x - o)) + 500$	500
F10: Shifted and Rotated Schaffer	-MM* -NS* -A* -LOH*		$L(\mathbf{X}) = \left(\frac{1}{D-1} \sum_{i=1}^{D-1} (\sqrt{s_i} (\sin(50.0s_i^{0.2}) + 1))\right)^2 s_i = \sqrt{x_i^2 + x_{i+1}^2} f(\mathbf{X}) = L\left(M\left(\frac{0.5(x - o)}{100}\right)\right) + 600$	600

* : MM: Multi-Modal, NS: Non-Separable, LOH: Local optima's number is huge, A: Asymmetrical, S: Shifted, SP: Separable, SC: Scalable, R:Rotated, parameters of o, z and M as the rotation operators are given in details CEC2017 database

** : All functions' formulations are given in CEC2017 database

* : MM: Multi-Modal, NS: Non-Separable, LOH: Local optima's number is huge, A: Asymmetrical, S: Shifted, SP: Separable, SC: Scalable, parameters of o, z and M as the rotation operators are given in details CEC2017 database

** : All functions' formulations are given in CEC2017 database

Table 6
Comparative results for BISA and other techniques.

Func.	Value	FA	TLBO	DSO	iPSO	ISA	BISA
F1	Mean	8.2258E-01	1.4561E-29	5.9987E-16	5.0401E-01	3.47E-01	0
	Std.	5.6698E-01	5.9174E-30	9.2356E-18	1.1250E-30	2.0982E-01	0
	Rank	6	2	3	4	5	1
F2	Mean	2.8876E-04	6.3678E-55	7.9034E-21	1.1131E-50	4.9132E-86	0
	Std.	2.2341E-09	4.9192E-57	5.4445E-22	2.3712E-53	8.3109E-87	0
	Rank	6	3	5	4	2	1
F3	Mean	8.8605E-12	5.5667E-86	6.0697E-18	7.015E-25	6.2227E-85	4.797E-113
	Std.	0.1419E-13	5.4101E-89	3.6489E-20	5.6624E-27	5.6427E-87	7.9631E-115
	Rank	6	2	5	4	3	1
F4	Mean	9.8004E-56	9.0899E-180	7.717E-188	9.9326E-165	3.4078E-189	0
	Std.	0.1419E-59	5.4101E-182	3.6489E-190	5.6624E-166	5.6427E-192	0
	Rank	6	4	3	5	2	1
F5	Mean	3.9024E+09	1.0932E+04	5.8021E+07	8.4109E+05	5.7632E+04	4.8932E+01
	Std.	1.5377E+04	8.2004E+02	3.8356E+04	1.2945E+02	1.2314E+02	7.9062E+00
	Rank	6	2	5	4	3	1
F6	Mean	7.6535E+6	1.5298E+03	9.9987E+07	9.8740E+6	2.9873E+03	1.9823E+02
	Std.	7.8898E+04	3.22E+02	1.2924E+04	4.2569E+03	1.0154E+02	3.6497E+01
	Rank	4	2	6	5	3	1
F7	Mean	6.9156E+05	2.4671E+01	3.8763E+04	1.2392E+02	-3.9012E+02	-3.9410E+02
	Std.	3.6495E+04	7.9887E+04	4.9277E+04	2.158E+06	6.3409E+02	8.015E+00
	Rank	6	3	5	4	2	1
F8	Mean	5.6734E+02	4.0932E+02	4.3093E+02	5.4234E+02	4.2345E+02	4.0100E+02
	Std.	7.8898E+02	3.22E+00	1.2924E+01	4.2569E+01	1.0154E+00	9.6497E-1
	Rank	6	2	4	5	3	1
F9	Mean	7.2398E+02	6.9834E+02	5.8724E+02	8.7653E+02	6.0376E+02	5.0043E+02
	Std.	6.3606E+02	2.449E+00	3.2852E+01	6.2483E+01	3.2223E+00	1.3488E-01
	Rank	5	4	2	6	3	1
F10	Mean	6.3023E+02	6.0153E+2	6.7823E+02	6.2309E+02	6.0124E+02	6.0000E+02
	Std.	1.4702E+02	3.3597E+00	1.4459E+01	1.9681E+01	1.7649E+00	0.0
	Rank	5	3	6	4	2	1

$$\alpha = \frac{\gamma}{2E_w}, \quad \beta = \frac{K - \gamma}{2E_D} \tag{19}$$

where, $\gamma = \sum_{i=1}^M \frac{\lambda_i}{\lambda_i + \alpha}$

In which λ_i are the eigenvalues of Hessian matrix defined as $H = \beta \nabla \nabla E_D$. In the next section, to obtain the optimal formulation for memory impact factor (ω), the governing posterior is maximized.

3.1.2. Posterior Maximization and Acquiring the Formulation

Considering the Eq. (12) the maximization is implemented on $S(W)$ as follows:

$$S(W) = \alpha E_w + \beta E_D = \frac{\beta}{2} (\Omega W - Q)^T (\Omega W - Q) + \frac{\alpha}{2} W^T W \tag{20}$$

By derivation respect to W ,

$$\begin{aligned} \frac{\partial(S(W))}{\partial W} &= \frac{\beta}{2} \left\{ \frac{\partial(\Omega W - Q)^T}{\partial W} \left((\Omega W - Q) + \frac{\partial(\Omega W - Q)^T}{\partial W} (\Omega W - Q) \right) \right\} + \alpha W \\ &= \frac{\beta}{2} \{ 2\Omega^T (\Omega W - Q) \} + \alpha W \\ &= \beta \Omega^T W \Omega - \beta \Omega^T Q + \alpha W = \beta \Omega^T \Omega W - \beta \Omega^T Q + \alpha W \end{aligned} \tag{21}$$

Implementing $\frac{\partial(S(W))}{\partial W} = 0$ criterion,

$$W = (\beta \Omega^T \Omega + \alpha)^{-1} \beta \Omega^T Q \tag{22}$$

Using Eq. (22) the *memory impact factor* can adaptively be adjusted. For more illustration, the pseudo code for the proposed BISA methods is given in Table 3.

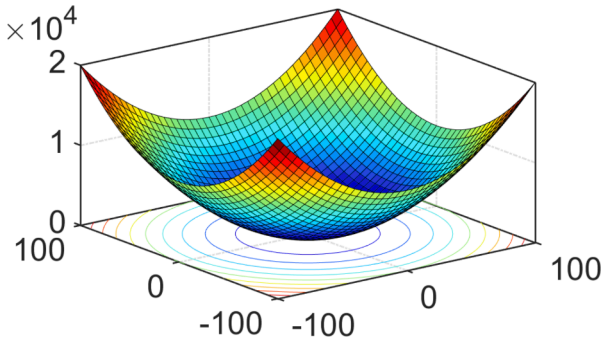
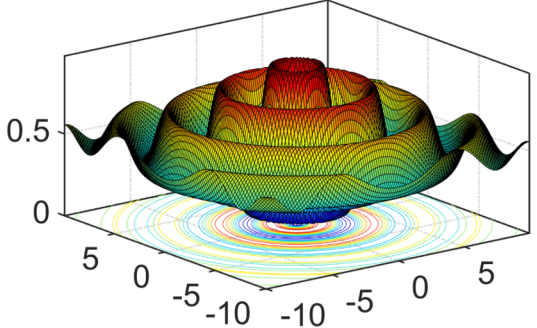
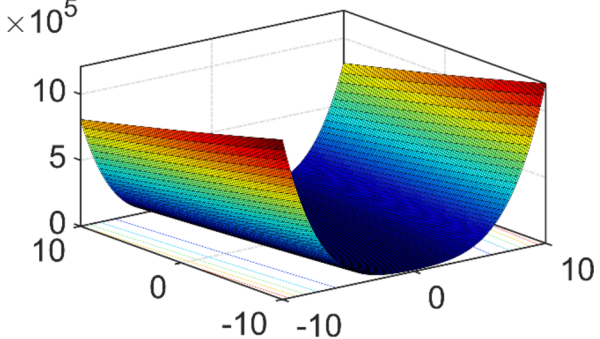
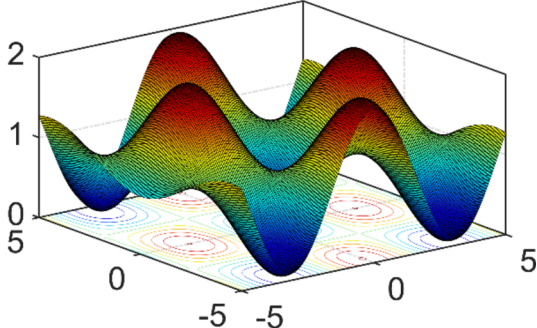
4. Numerical Tests

In this section the performance of the proposed BISA is tested on a suite of unconstrained mathematical functions and constrained structural problems with both discrete and continuous variables. The algorithms are run on the computer equipped with the intel™-i7 CPU and 12 MB of installed RAM. It should be noted that, the main purpose of the current study is to evaluate achieved enhancements for BISA over its parent method (i.e. ISA), but to provide more insight into BISA's performance, in addition to ISA, extra four well-established methods (based on author knowledge) are also selected to make comparison. Parameters setting for applied methods are given in Table 4.

4.1. Unconstrained Mathematical Functions

The current section is devoted to comparatively assess the accuracy level, stability, convergence rate, complexity and diversity change scheme of the proposed BISA on a suite of unconstrained mathematical functions. All selected functions are initiated in $[-100, 100]^D$, where D is the problem's dimension which is taken as 30 for all functions. To prevent any premature convergence condition, selected algorithms are run for $10000 * D$ of Objective Function Evaluations (OFEs).

Table 7
Benchmark functions and their properties.

Function	Properties	Schematic Plot	Formulation	min
F11: Sphere	-UM* -NS*		$f(\mathbf{X}) = \sum_{i=1}^2 x_i^2$	0
F12: Schaffer	-UM* -NS* -LOH*		$f(\mathbf{X}) = 0.5 + \frac{\sin^2(\sqrt{x_1^2 + x_2^2}) - 0.5}{(1 + 0.001(x_1^2 + x_2^2))^2}$	0
F13: Rosenbrock	-UM* -S*		$f(\mathbf{X}) = \sum_{i=1}^2 100(x_{i-1} + x_i^2)^2 + (x_i - 1)^2$	0
F14: Griewank	-UM* -NS* -LOH*		$f(\mathbf{X}) = \sum_{i=1}^n \frac{x_i^2}{4000} + \prod_{i=1}^n \cos\left(\frac{x_i}{\sqrt{i}}\right)$	0

* : UM: Uni-Modal, NS: Non-Separable, LOH: Local optima's number is huge

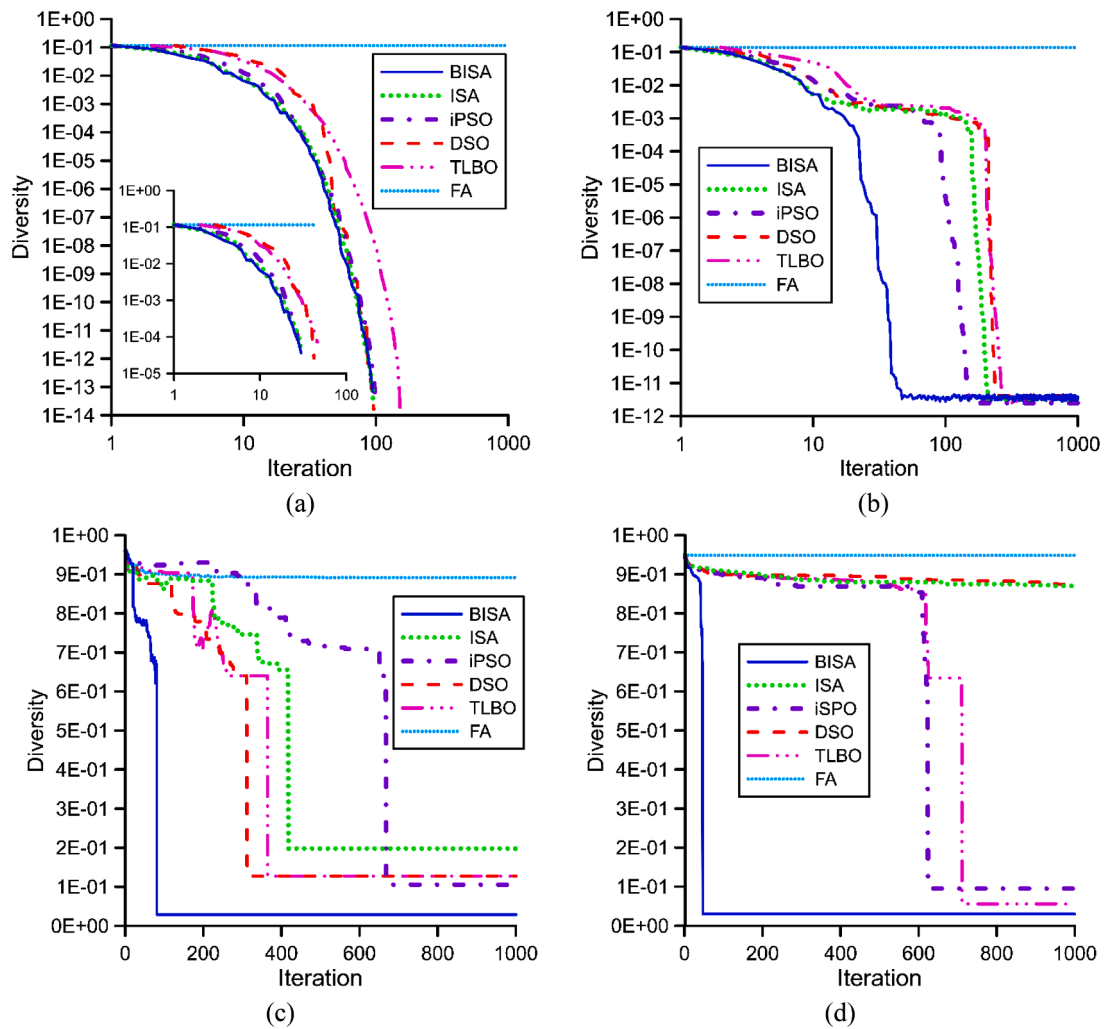


Fig. 1. Diversity diagrams for (a) F11 and (b) F12 (c) F13 and (d) F14 functions.

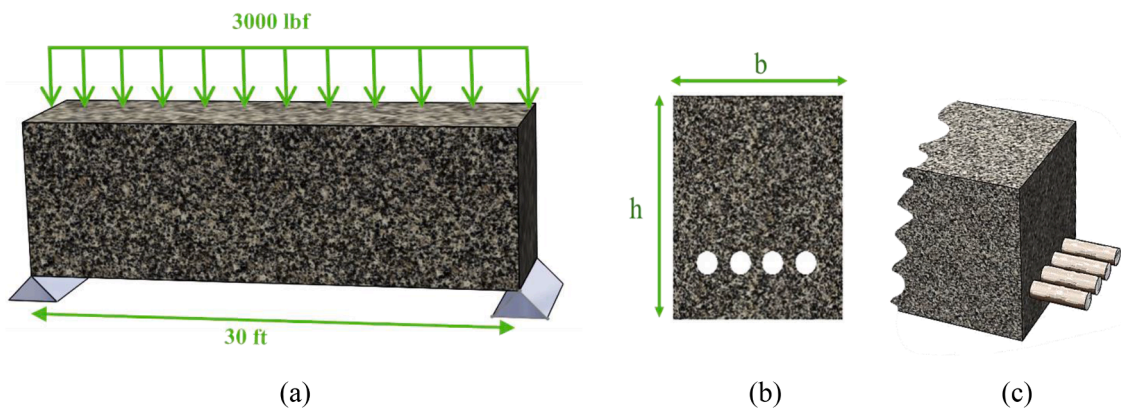


Fig. 2. Reinforced concrete beam system (a) loading condition, (b) section view (c) reinforcing details.

Table 8
Objective function and constraints of the concrete beam problem.

Function	Mathematical formulation
Objective function	$f(A_s, b, h) = 2.9A_s + 0.6bh$
Constraints	$g_1(A_s, b, h) = 7.375 \frac{A_s^2}{b} - A_s h + 180 \leq 0$ $g_2(b, h) = \frac{h}{b} - 4 \leq 0$
Variable's bounds	$5 \leq b \leq 10$ $A_s = [6, 6.16, 6.32, 6.6, 7.0, 7.11, 7.2, 7.8, 7.9, 8.0, 8.4]$ $h = [28, 29, 30, \dots, 40]$

4.1.1. Accuracy, Stability and Complexity Analyses

In this section, the accuracy and stability of the proposed BISA are verified on optimizing ten different mathematical functions. Some of these function are selected from CEC2017 database [55]. Selected functions have different properties which can challenge the algorithm from different aspects. For example, while the unimodal functions demand the higher level of exploration behavior, those with multimodal and noisy domains require higher level of exploitation search behavior. The list of these functions, their 2D schematic shape, main properties, formulation, and expected global optimum points are tabulated in Table 5.

Based on the acquired numerical results given in Table 6., the BISA can comparatively find more accurate solutions. Also, the given standard deviation (Std.) values show that the BISA shows superior performance in the term of stability. These outcomes indicate that the Bayesian regulator mechanism performs well and by reducing ineffective iterations (iterations without improvements) increases the efficiency of the BISA algorithm.

4.1.2. Diversity Analysis

In the conventional approach, the convergence history diagrams just trace of the best agent of the population during the optimization process. However, it would be more realistic if the situation of the whole population were taken into account to measure the convergence of the algorithm. In this regard, in the current section the convergence behavior of the proposed BISA is assessed using the diversity index defined in Eq. (23) [41].

$$Diversity(t) = \frac{1}{N|L|} \sum_{i=1}^N \sqrt{\sum_{j=1}^D (x_i^j - \bar{x}^j)^2} \tag{23}$$

where, the current condition of population shown by t , N indicates the population number; D designates the problem dimension, L gives the longest diagonal length of search domain. Also, x_i^j is the i th agent's j th component, and \bar{x}^j is the mean value of all j th components of the population. The selected benchmark functions for convergence test are

Table 9
The optimal result for concrete beam problem.

Parameter	FA	TLBO	DSO	iPSO	ISA	BISA
A_s (in ²)	7.2	6.6	6.16	6.16	6.32	6.32
b (in)	8.0451	8.4952	8.75	8.75	8.6371	8.500
h (in)	32	33	35	34	34	34
g_1	-0.0224	-0.1155	-0.0224	0.00	-0.0635	0.00
g_2	-2.8779	0.0159	-3.6173	-3.6173	-0.7745	-0.2241
$f(X)$						
Best	366.1459	362.2455	364.8541	364.8540	362.0020	359.2080
Mean	378.13	369.20	368.7193	368.208	366.227	359.2080
Std.	8.29	2.54	5.78	4.02	4.34	0.00
OFEs	2,850	3,120	3,880	2,255	2,200	650

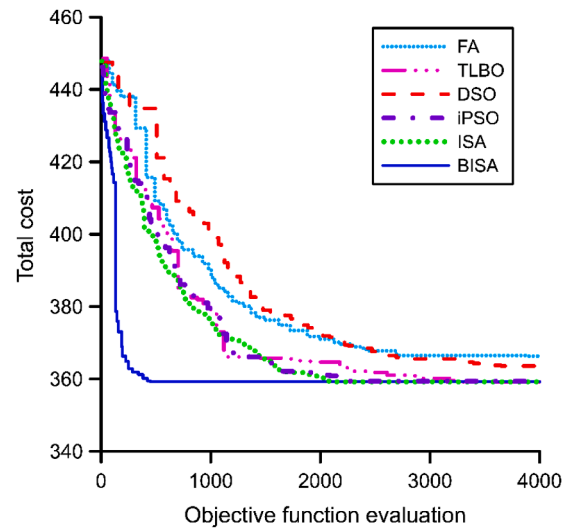


Fig. 3. The convergence history for concrete beam problem.

plotted in Table 7.

Fig. 1 shows the attained diversity change diagrams. To create a better perception, the axes are logarithmically scaled in these diagrams. Based addressed outcomes the proposed BISA shows the most rapid convergence rate in comparison with regular ISA and other selected methods.

4.2. Constrained Structural Optimization Problems

This section is devoted to comparatively assess the search performance of the proposed BISA on handling the structural optimization problems with dynamic and static constraints including both discrete and continuous variables. To prevent any premature convergences, all problems are run for 30 times.

4.2.1. Manufacturing Cost Minimization of the Reinforced Concrete Beam

In this example, the minimization of the manufacturing cost of the concrete beam is targeted. In this regard, to obtain a feasible system, the beam not only should be flexural designed but also from the practical view some constraints should be implemented through the design process. The beam system and its loading condition are demonstrated in Fig. 2.

This problem includes three decision variables as rebar areas ($x_1=A_s$), width ($x_2=b$) and height ($x_3=h$) of the beam. Also, the stability of the system which is declared with Eq. (24) should be satisfied. In this formulation the ultimate internal moment of the beam is

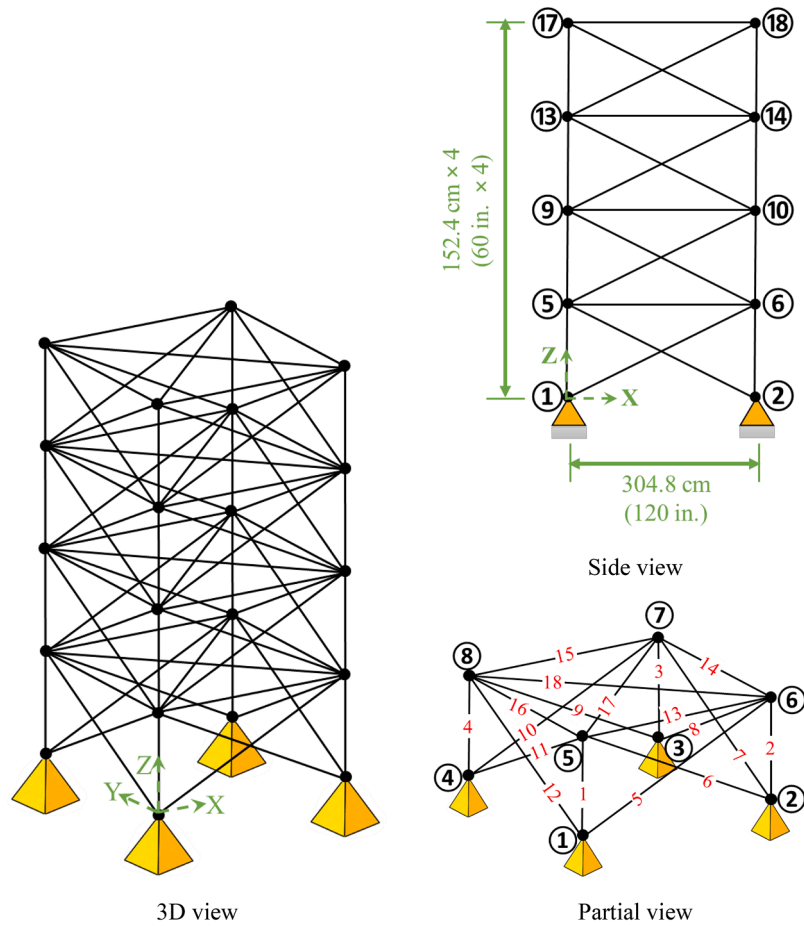


Fig. 4. The 72-bar truss structure.

Table 10
Obtained optimal results for the 72-bar truss structure

Design Variables (in ²)	Optimal cross-sectional area					
	FA	TLBO	DSO	iPSO	ISA	BISA
A ₁ -A ₄	1.9	1.7	1.9	1.9	1.9	1.9
A ₅ -A ₁₂	0.5	0.5	0.5	0.5	0.5	0.5
A ₁₃ -A ₁₆	0.1	0.1	0.1	0.1	0.1	0.1
A ₁₇ -A ₁₈	0.1	0.1	0.1	0.1	0.1	0.1
A ₁₉ -A ₂₂	1.2	1.3	1.3	1.3	1.3	1.3
A ₂₃ -A ₃₀	0.5	0.5	0.5	0.5	0.5	0.5
A ₃₁ -A ₃₄	0.1	0.1	0.1	0.1	0.1	0.1
A ₃₅ -A ₃₆	0.1	0.1	0.1	0.1	0.1	0.1
A ₃₇ -A ₄₀	0.5	0.5	0.5	0.5	0.5	0.5
A ₄₁ -A ₄₈	0.5	0.5	0.5	0.5	0.5	0.5
A ₄₉ -A ₅₂	0.1	0.1	0.1	0.1	0.1	0.1
A ₅₃ -A ₅₄	0.1	0.1	0.1	0.1	0.1	0.1
A ₅₅ -A ₅₈	0.2	0.2	0.2	0.2	0.2	0.2
A ₅₉ -A ₆₆	0.6	0.5	0.6	0.6	0.6	0.5
A ₆₇ -A ₇₀	0.4	0.5	0.4	0.4	0.4	0.4
A ₇₁ -A ₇₂	0.6	0.6	0.5	0.5	0.5	0.6
Best Weight (lb)	379.9	381.9	380.6	380.6	380.6	379.6
Mean weight (lb)	382.2	382.2	383.9	381.7	382.5	379.8
Std. (lb)	1.78	1.01	3.21	2.31	2.12	1.04
OFEs	10,620	14,840	13,200	11,200	10,040	5,800

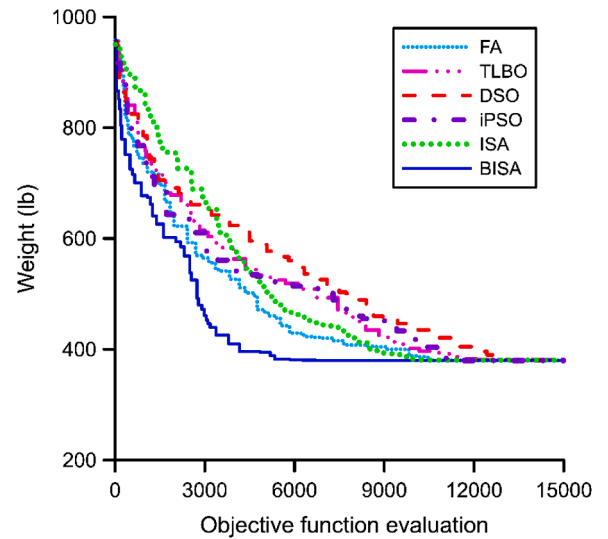
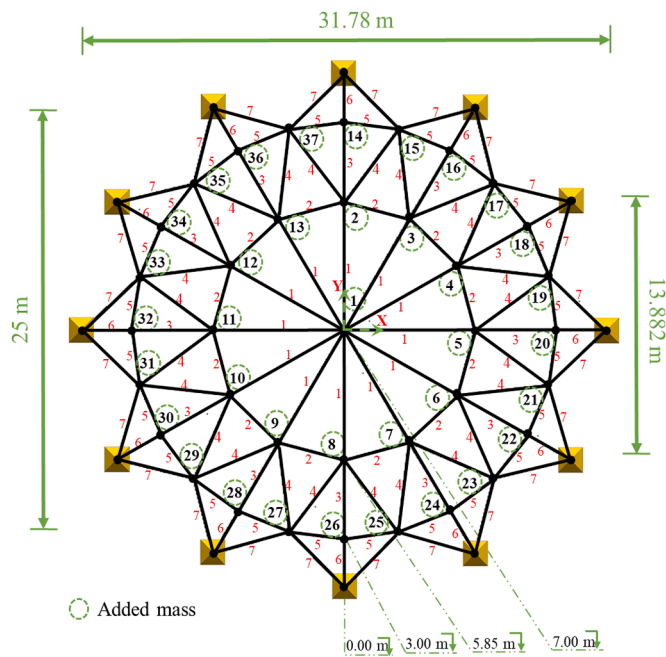
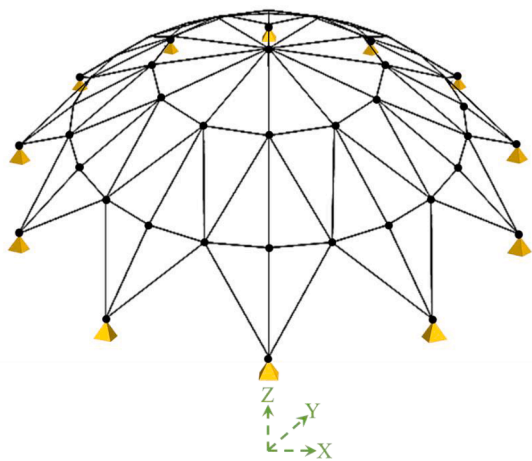


Fig. 5. The convergence history for 72-bar truss structure.



a) Top view



b) 3D view

Fig. 6. The 120-bar dome structure.

abbreviated by M_{ib} and σ_y and σ_c indicate the yielding stress of the steel bars and allowable compressive stress of concrete, respectively. External moments caused by the dead and live loads are shown by M_d and M_l respectively. Also, M_d and M_l are respectively taken as 1350 kip.in and 2700 kip.in. and σ_y and σ_c are set as 50 ksi and 5 ksi, respectively. The objective function, constraints and decision variable bounds of this problem is given in Table 8. Acquired optimal results for this problem are given in Table 9. Also, the convergence history for optimization process are plotted in Fig. 3. Based on the given data, BISA, TLBO and iPSO can find the same optimal solution. However, number of Objective Function Evaluations (OFEs) indicate that BISA find the solution in considerably lower computational cost. Also, the values of standard deviations reveal that BISA shows the most stable behavior.

$$M_u = 0.72 A_s \sigma_y h \left(1 - \frac{0.59 A_s \sigma_y}{0.8 b h \sigma_c} \right) \geq 1.4 M_d + 1.7 M_l \quad (24)$$

4.2.2. Weight minimization of a 72-bar spatial truss system with discrete variable

In the current section the search capability of the BISA is assessed on handling a constrained structural optimization problem. To meet this aim, the weight minimization of 72-bar spatial truss system shown in Fig. 4 is pointed. In this system the nodal displacements in all principal directions is restricted to ± 0.25 in. The maximum tensile and compressive stresses for all members are restricted up to ± 25 ksi. Maintain the symmetry of the system, structural members are categorized into 16 groups. The module of elasticity and density of the material

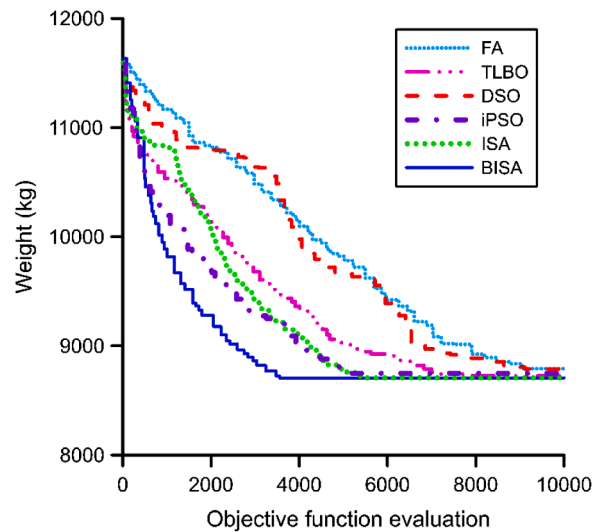


Fig. 7. The convergence history for 120-bar dome problem.

Table 11
The optimal result for 120-bar dome structure.

Design Variables	Optimal cross-sectional area (cm ²)					
	FA	TLBO	DSO	iPSO	ISA	BISA
A ₁	19.607	20.263	20.0325	18.9791	20.263	19.5093
A ₂	41.290	39.294	38.2935	41.0046	39.294	40.3911
A ₃	11.136	9.989	11.7403	10.6124	9.989	10.6066
A ₄	21.025	20.563	21.9118	21.8776	20.563	21.1368
A ₅	10.060	9.603	10.2	10.7519	9.603	9.8134
A ₆	12.758	11.738	10.9328	12.4286	11.738	11.7798
A ₇	15.414	15.877	14.6337	13.7772	15.877	14.8192
Best weight (kg)	8790.48	8724.97	8789.50	8748.21	8724.97	8707.28
Mean weight (kg)	8800.18	8732.01	8901.39	8751.87	8732.52	8707.49
Std. (kg)	8.90	4.91	8.01	3.87	4.02	0.01
OFEs	9,050	8,710	9,120	5,010	5,380	3,550

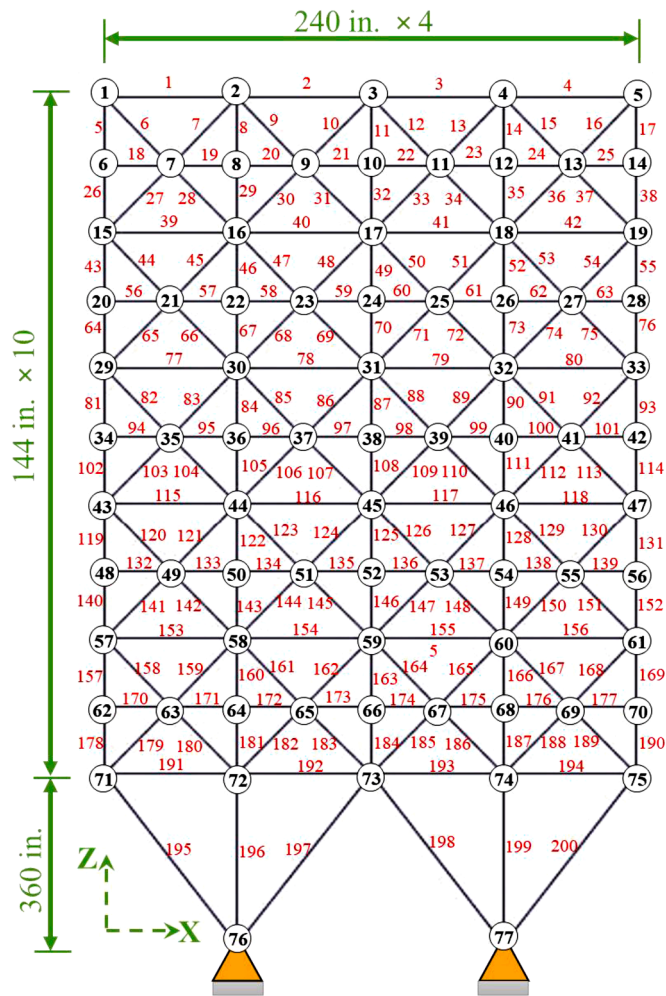


Fig. 8. The 200-bar planar truss structure.

are taken as 10,000 ksi and 0.1 lb/in³, respectively. Node 17 of this structure is subjected to $P_x=5$, $P_y=5$ and $P_z=-5$ kips loads. Upper and lower bounds for sizing variables (cross-sectional areas) are restricted to 0.01 in² and 10 in², respectively.

Acquired results are tabulated in Table 10. Based on the presented outcomes, results given by BISA are superior in the term of both accuracy and stability. Also, based on the convergence history of the optimization process given in Fig. 5, the proposed BISA provides the most rapid convergence history. Furthermore, based on the reported number of OFEs, the proposed BISA fairly demand 50% less of computational cost in comparison with other methods. It is notable that, this problem are solved in Ref. [56] with different set of the decision variables, as well.

4.2.3. Weight minimization of a 120-bar dome structure with dynamic constraints

The 120-bar dome structure demonstrated in Fig. 6 is solved for weight minimization with multiple natural frequencies limitations. The

Table 12 Grouping of 200-bar planar truss structure

Group No.	Group members
1	1-2-3-4
2	5-8-11-14-17
3	19-20-21-22-23-24
4	18-25-56-63-94-101-132-139-170-177
5	26-29-32-35-38
6	6-7-9-10-12-13-15-16-27-28-30-31-33-34-36-37
7	39-40-41-42
8	43-46-49-52-55
9	57-58-59-60-61-62
10	64-67-70-73-76
11	44-45-47-48-50-51-53-54-65-66-68-69-71-72-74-75
12	77-78-79-80
13	81-84-87-90-93
14	95-96-97-98-99-100
15	102-105-108-111-114
16	82-83-85-86-88-89-91-92-103-104-106-107-109-110-112-113
17	115-116-117-118
18	119-122-125-128-131
19	133-134-135-136-137-138
20	140-143-146-149-152
21	120-121-123-124-126-127-129-130-141-142-144-145-147-148-150-151
22	153-154-155-156
23	157-160-163-166-169
24	171-172-173-174-175-176
25	178-181-184-187-190
26	158-159-161-162-164-165-167-168-179-180-182-183-185-186-188-189
27	191-192-193-194
28	195-197-198-200
29	196-199

Table 13 loading conditions for 200-bar planar truss structure

Loading condition	Nodes	F _x (kips)	F _y (kips)	F _z (kips)
I	1, 6, 15, 20, 29, 34, 43, 48, 57, 62	1	0	0
II	1-6, 8, 10, 12, 14-20, 22, 24, 26, 28-34, 36, 38, 40, 42-48, 50, 52, 54, 56-62, 64, 66, 68, 70-75	0	-10	0
III	Loading conditions I and II acting together			

elasticity modulus and density of the material are 210 GPa and 7971.81 kg/m³, respectively. Maintaining symmetry, the structural members, as shown in Fig. 6, are categorized into 7 independent groups. Nodes number 1, 2-13 and 14-37 are respectively subjected to a non-structural mass as 3000 kg, 500 kg and 100 kg. This problem restricted by two inequality for two first natural frequencies as $\Phi_1 \geq 9$ Hz and $\Phi_2 \geq 11$ Hz. Sizing decision continuous variables lower and upper bounds are set as 1 cm² and 129.3 cm², respectively.

The achieved optimal solutions are reported in Table 11 and the convergence diagrams for all tested methods are plotted in Fig. 7. There are no any constraint violations in all reported results. Based on the given outcomes, the proposed BISA is superior in the terms of accuracy and convergence rate. Also, the statistical data reveals that BISA shows the most stable behavior. These feedbacks indicate that the Bayesian regulator module can work properly to reduce the number of ineffective iteration and increase the accuracy and efficiency of the algorithm.

Table 14
The optimal result for 200-bar dome structure

Design Variables	Optimal cross-sectional areas (in ²)						
	FA	TLBO	DSO	iPSO	NMA*	ISA	BISA
1	0.100	0.100	0.100	0.100	0.100	0.100	0.100
2	2.142	0.954	0.954	0.954	0.954	0.954	0.954
3	0.347	0.347	0.347	0.347	0.347	0.347	0.347
4	0.100	0.100	0.100	0.100	0.100	0.100	0.100
5	3.131	2.142	2.142	2.142	2.142	2.142	2.142
6	0.347	0.347	0.347	0.347	0.347	0.347	0.347
7	4.805	0.100	0.100	0.100	0.100	0.100	0.100
8	0.539	3.131	3.131	3.131	3.131	3.131	3.131
9	0.347	0.100	0.100	0.100	0.100	0.100	0.100
10	5.952	4.805	4.805	4.805	4.805	4.805	4.805
11	0.100	0.440	0.440	0.440	0.539	0.440	0.440
12	6.572	0.100	0.100	0.100	0.100	0.100	0.100
13	0.954	5.952	5.952	5.952	5.952	5.952	5.952
14	0.440	0.100	0.100	0.100	0.100	0.100	0.100
15	8.525	6.572	6.572	6.572	6.572	6.572	6.572
16	0.100	0.539	0.539	0.539	0.539	0.539	0.539
17	9.300	0.440	0.347	0.347	0.440	0.347	0.440
18	0.954	8.525	8.525	8.525	8.525	8.525	8.525
19	1.081	0.347	0.100	0.100	0.100	0.100	0.100
20	13.33	9.300	9.300	9.300	9.300	9.300	9.300
21	0.539	0.954	0.954	0.954	0.954	0.954	0.954
22	14.29	0.539	1.174	0.954	0.347	0.539	0.347
23	2.142	13.33	13.33	13.33	13.33	13.33	13.33
24	3.813	0.100	0.100	0.100	0.100	0.100	0.100
25	8.525	13.33	13.33	13.33	13.330	13.33	13.33
26	17.17	1.333	1.333	1.333	1.081	1.174	1.174
27	0.100	5.952	5.952	5.952	5.952	5.952	5.952
28	2.142	10.850	10.850	10.850	10.850	10.850	10.850
29	0.347	14.290	14.290	14.290	14.290	14.290	14.290
Best Weight (lb)	27,858.50	27,614.30	27,717.52	27,610.63	27,125.07	27,146.87	27,119.98
Mean Weight (lb)	28,735.12	27,912.45	28,144.87	27,878.36	27,575.11	27,605.58	27,206.85
Std. (lb)	1,256.36	485.25	586.47	447.87	221.72	220.89	145.25
OFEs	11,400	12,510	14,550	9,870	10,000	8,550	5,820

* : The results for Newton Metaheuristic Algorithm (NMA) are taken from Ref. [57].

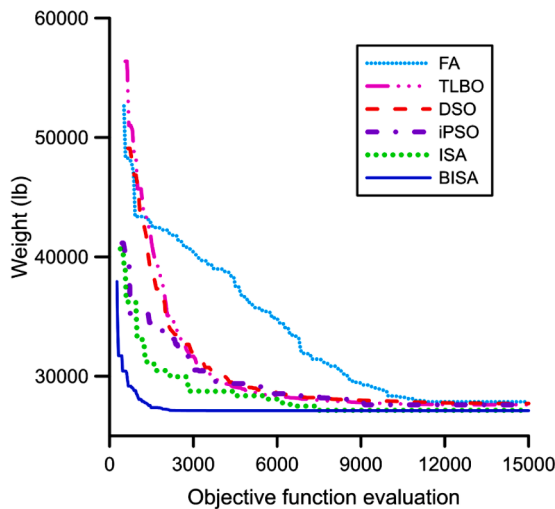


Fig. 9. The convergence history for 200-bar dome problem.

4.2.4. Weight minimization of a 200-bar truss structure with discrete variables

In this section, the 200-bar planar truss structure, presented in Fig. 8 is studied for weight minimization. The density and modulus of elasticity of the material are 0.283 lb/in³ and 30 Msi, respectively. Allowable stress for the both tensile and compressive members is ±10.0 ksi. The members of the truss are divided to 29 independent groups as given in Table 12. The truss is considered to be exposed to three different loading conditions, those are given in Table 13. The design cross-sectional variables are selected from a discrete set as: {0.100, 0.347, 0.440, 0.539, 0.954, 1.081, 1.174, 1.333, 1.488, 1.764, 2.142, 2.697, 2.800, 3.131, 3.565, 3.813, 4.805, 5.952, 6.572, 7.192, 8.525, 9.300, 10.850, 13.330, 14.290, 17.170, 19.180, 23.680, 28.080, 33.700}in². The attained optimal results for BISA and other selected methods are provided in Table 14. The convergence history diagrams for the optimization process for selected methods are given in Fig. 9. The proposed BISA can find the lightest structural system demanding the lowest number of OFEs, especially in comparison with its parent method (i.e. ISA), and this indicates that the Bayesian regulator module of the method works proper in reducing the computational cost and improving the accuracy of the algorithm.

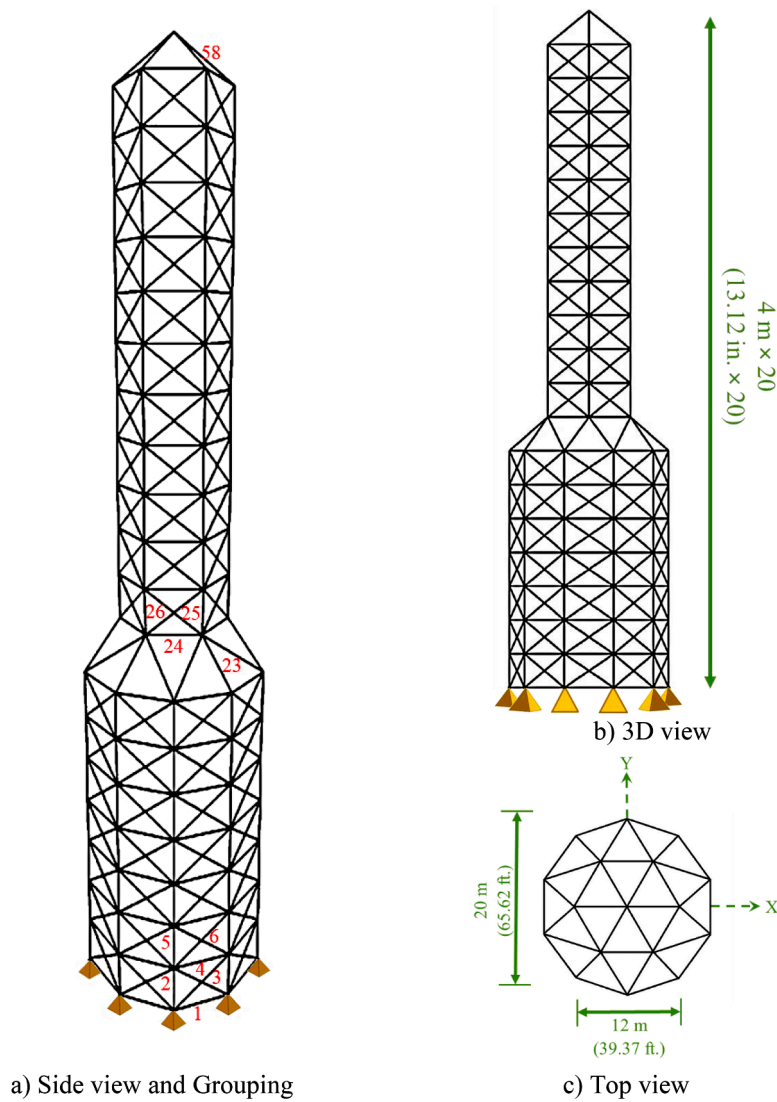


Fig. 10. The 582-bar truss tower structure.

4.2.5. Weight minimization of a 582-bar truss tower with extended grouping

As the last example, the weight minimization of the 582-bar spatial truss tower shown in Fig. 10 is considered. Maintaining the symmetry, the members of this structure are categorized into 58 independent groups [14]. Given tower system is subjected to three different loading conditions as below:

- I Each node is subjected to -6.75 kips load in the vertical direction
- II Each node is subjected to 1.12 kips load in the x- direction (horizontally)
- III Each node is subjected to 1.12 kips load in the y- direction (vertically)

As given in Table 15, the sizing variables are picked from a discrete set of predefined W-shape profiles given in AISC-ASD database. Accordingly, the upper and lower bound for sizing variables are restricted as 215.0 in² (1387.09 cm²) and 6.16 in² (39.74 cm²), respectively. All nodal displacement is limited up to 3.15 in (8 cm). For all structural members, considering the buckling criterion, stress is limited based on the AISC-ASD89 code as follows:

$$\begin{cases} \sigma_i^+ = 0.6F_y & \sigma_i \geq 0 \\ \sigma_i^- & \sigma_i < 0 \end{cases} \quad (25)$$

Table 15
Discrete cross-sections available for the sizing variables of the 582-bar tower problem.

W-shape profile list taken from AISC code						
W27 × 178	W21 × 122	W18 × 50	W14 × 455	W14 × 74	W12 × 136	W10 × 77
W27 × 161	W21 × 111	W18 × 46	W14 × 426	W14 × 68	W12 × 120	W10 × 68
W27 × 146	W21 × 101	W18 × 40	W14 × 398	W14 × 61	W12 × 106	W10 × 60
W27 × 114	W21 × 93	W18 × 35	W14 × 370	W14 × 53	W12 × 96	W10 × 54
W27 × 102	W21 × 83	W16 × 100	W14 × 342	W14 × 48	W12 × 87	W10 × 49
W27 × 94	W21 × 73	W16 × 89	W14 × 311	W14 × 43	W12 × 79	W10 × 45
W27 × 84	W21 × 68	W16 × 77	W14 × 283	W14 × 38	W12 × 72	W10 × 39
W24 × 162	W21 × 62	W16 × 67	W14 × 257	W14 × 34	W12 × 65	W10 × 33
W24 × 146	W21 × 57	W16 × 57	W14 × 233	W14 × 30	W12 × 58	W10 × 30
W24 × 131	W21 × 50	W16 × 50	W14 × 211	W14 × 26	W12 × 53	W10 × 26
W24 × 117	W21 × 44	W16 × 45	W14 × 193	W14 × 22	W12 × 50	W10 × 22
W24 × 104	W18 × 119	W16 × 40	W14 × 176	W12 × 336	W12 × 45	W8 × 67
W24 × 94	W18 × 106	W16 × 36	W14 × 159	W12 × 305	W12 × 40	W8 × 58
W24 × 84	W18 × 97	W16 × 31	W14 × 145	W12 × 279	W12 × 35	W8 × 48
W24 × 76	W18 × 86	W16 × 26	W14 × 132	W12 × 252	W12 × 30	W8 × 40
W24 × 68	W18 × 76	W14 × 730	W14 × 120	W12 × 230	W12 × 26	W8 × 35
W24 × 62	W18 × 71	W14 × 665	W14 × 109	W12 × 210	W12 × 22	W8 × 31
W24 × 55	W18 × 65	W14 × 605	W14 × 99	W12 × 190	W10 × 112	W8 × 28
W21 × 147	W18 × 60	W14 × 550	W14 × 90	W12 × 170	W10 × 100	W8 × 24
W21 × 132	W18 × 55	W14 × 500	W14 × 82	W12 × 152	W10 × 88	W8 × 21

$$\sigma_i^- = \begin{cases} \left[\left(1 - \frac{\lambda_i^2}{2C_c^2} \right) F_y / \left(\frac{5}{3} + \frac{3\lambda_i}{8C_c} - \frac{\lambda_i^3}{8C_c^3} \right) \right] & \text{for } \lambda_i < C_c \\ \frac{12\pi^2 E}{23\lambda_i^2} & \text{for } \lambda_i \geq C_c \end{cases} \quad (26)$$

where, the compressive and tensile stresses are shown by σ_i^- and σ_i^+ , respectively. For the compressive members, allowable stress (i.e. σ_i^-) depends on their slenderness ratio (λ). The critical slenderness is demonstrated by C_c and defined as follows:

$$C_c = \sqrt{\frac{2\pi^2 E}{F_y}} \quad (27)$$

Based on the AISC-ASD code, for compressive and tensile members, maximum allowable slenderness ratios should be less or equal than 300 and 200, respectively. Slenderness and its limitations are shown as below:

$$\lambda_i = \frac{k_i l_i}{r_i} \leq \begin{cases} 300 & \text{for tension members} \\ 200 & \text{for compression members} \end{cases} \quad (28)$$

in which l_i , r_i and λ_i , for the i th member, designate the length of member, radius of gyration and slenderness ratio, respectively. For compression members, if given slenderness ratio is violated the maximum allowable value for stress must not be exceeded from $\left(\frac{12\pi^2 E}{23\lambda_i^2} \right)$ value (AISC-ASD89).

Achieved numerical results are reported in Table 16. Based on reported outcomes, the proposed BISA found the lightest structural system in comparison with other methods. The convergence histories for optimization process are presented in Fig. 11. Also, BISA considerably demands the lowest number of OFEs. It should be noted that, given the complexity of the problem, this amount of OFEs reduction has a significant effect in decreasing the computational cost.

5. Discussion on the Proposed Bayesian Mechanism

The proposed Bayesian formula dynamically updates the memory impact factor (ω) based on the collecting evidence during the optimization process. As described before (see section 3.1.2) activation period (k) specifies that the how often Bayesian regulator mechanism should be activated (i.e. it should be activated in each k iterations). So, if k is small, the contribution of the memory concept is updated more frequently. However, if k is high, the contribution of the memory concept is updated slower. So, to optimize the computational cost, it would be better to determine an optimal value for the activation period (k).

For this aim, the sphere function is selected as the unconstrained problem, and the 72-bar truss structure is selected as a constrained problem. The required iterations to reach the same optimal result for different values of k are given in Table 17. Based on this table, the $k=10$ provides the lowest computational cost for both selected problems. So, this value is recommended for activation period of the proposed Bayesian formulation. It should be noted that, this parameter is also tested on other structural and mathematical problems and the general pattern is in the agreement with given table.

To give a general perspective about working mechanism of the proposed Bayesian regulating strategy, in Fig. 12 the memory impact factor (ω) changes history during the optimization process are given for sphere function and 72-bar truss structure weight minimization problems. According to these diagrams the values of ω is permanently tuned. Also, the linear diagrams that are fitted for both test problems indicate that, at early iterations the exploration search behavior is dominant, while as the search process progresses, its effect is gradually reduced and the exploitation search behavior gains prevailing.

6. Conclusion

The current study deals with developing a new forecasting Bayesian strategy to enhance the search capability of Interactive Search

Table 16
Optimal results for the 582-bar tower problem with 58 groups

Design Variables	Optimal cross-sectional areas					
	FA	TLBO	DSO	iPSO	ISA	BISA
1	W12 × 22 (6.48)	W12 × 22 (6.48)	W8 × 24 (7.08)	W8 × 21 (6.16)	W8 × 21 (6.16)	W8 × 21 (6.16)
2	W27 × 102 (30)	W10 × 88 (25.9)	W10 × 88 (25.9)	W24 × 84 (24.7)	W24 × 84 (24.7)	W24 × 84 (24.7)
3	W8 × 24 (7.08)	W8 × 24 (7.08)	W8 × 24 (7.08)	W8 × 24 (7.08)	W8 × 24 (7.08)	W8 × 24 (7.08)
4	W12 × 22 (6.48)	W12 × 22 (6.48)	W12 × 22 (6.48)	W8 × 21 (6.16)	W8 × 21 (6.16)	W8 × 21 (6.16)
5	W10 × 88 (25.9)	W16 × 89 (26.2)	W16 × 89 (26.2)	W14 × 74 (21.8)	W14 × 74 (21.8)	W14 × 74 (21.8)
6	W8 × 24 (7.08)	W8 × 24 (7.08)	W8 × 24 (7.08)	W8 × 24 (7.08)	W8 × 24 (7.08)	W8 × 24 (7.08)
7	W8 × 21 (6.16)	W8 × 21 (6.16)	W8 × 21 (6.16)	W8 × 21 (6.16)	W8 × 21 (6.16)	W8 × 21 (6.16)
8	W18 × 71 (20.8)	W18 × 71 (20.8)	W18 × 71 (20.8)	W18 × 71 (20.8)	W18 × 71 (20.8)	W18 × 71 (20.8)
9	W8 × 24 (7.08)	W8 × 24 (7.08)	W8 × 24 (7.08)	W8 × 24 (7.08)	W8 × 24 (7.08)	W8 × 24 (7.08)
10	W8 × 21 (6.16)	W8 × 21 (6.16)	W8 × 21 (6.16)	W8 × 21 (6.16)	W8 × 21 (6.16)	W8 × 21 (6.16)
11	W16 × 57 (16.8)	W12 × 50 (14.7)	W12 × 50 (14.7)	W12 × 50 (14.7)	W12 × 50 (14.7)	W12 × 50 (14.7)
12	W8 × 24 (7.08)	W8 × 24 (7.08)	W8 × 24 (7.08)	W8 × 24 (7.08)	W8 × 24 (7.08)	W8 × 24 (7.08)
13	W12 × 22 (6.48)	W12 × 22 (6.48)	W12 × 22 (6.48)	W8 × 21 (6.16)	W8 × 21 (6.16)	W8 × 21 (6.16)
14	W16 × 57 (16.8)	W12 × 50 (14.7)	W12 × 50 (14.7)	W12 × 50 (14.7)	W12 × 50 (14.7)	W12 × 50 (14.7)
15	W8 × 24 (7.08)	W8 × 24 (7.08)	W8 × 24 (7.08)	W8 × 24 (7.08)	W8 × 24 (7.08)	W8 × 24 (7.08)
16	W8 × 21 (6.16)	W8 × 21 (6.16)	W8 × 21 (6.16)	W8 × 21 (6.16)	W8 × 21 (6.16)	W8 × 21 (6.16)
17	W12 × 50 (14.7)	W12 × 45 (13.2)	W12 × 45 (13.2)	W12 × 45 (13.2)	W12 × 45 (13.2)	W12 × 45 (13.2)
18	W8 × 24 (7.08)	W8 × 24 (7.08)	W8 × 24 (7.08)	W8 × 24 (7.08)	W8 × 24 (7.08)	W8 × 24 (7.08)
19	W8 × 21 (6.16)	W8 × 21 (6.16)	W8 × 21 (6.16)	W8 × 21 (6.16)	W8 × 21 (6.16)	W8 × 21 (6.16)
20	W16 × 36 (10.6)	W16 × 36 (10.6)	W16 × 36 (10.6)	W16 × 36 (10.6)	W16 × 36 (10.6)	W16 × 36 (10.6)
21	W8 × 21 (6.16)	W8 × 21 (6.16)	W8 × 21 (6.16)	W8 × 21 (6.16)	W8 × 21 (6.16)	W8 × 21 (6.16)
22	W10 × 68 (20)	W10 × 68 (20)	W10 × 68 (20)	W10 × 68 (20)	W10 × 68 (20)	W10 × 68 (20)
23	W18 × 76 (22.3)	W18 × 76 (22.3)	W18 × 76 (22.3)	W14 × 61 (17.9)	W18 × 76 (22.3)	W14 × 61 (17.9)
24	W10 × 88 (25.9)	W10 × 68 (20)	W10 × 68 (20)	W18 × 76 (22.3)	W12 × 65 (19.1)	W18 × 76 (20)
25	W24 × 68 (20.1)	W24 × 68 (20.1)	W24 × 68 (20.1)	W21 × 83 (24.3)	W24 × 68 (20.1)	W21 × 83 (20.1)
26	W12 × 40 (11.8)	W12 × 40 (11.8)	W12 × 40 (11.8)	W12 × 40 (11.8)	W12 × 40 (11.8)	W12 × 40 (11.8)
27	W8 × 21 (6.16)	W8 × 21 (6.16)	W8 × 21 (6.16)	W8 × 21 (6.16)	W8 × 21 (6.16)	W8 × 21 (6.16)
28	W27 × 102 (30)	W18 × 76 (22.3)	W18 × 76 (22.3)	W18 × 76 (22.3)	W14 × 61 (17.9)	W18 × 76 (18.3)
29	W10 × 22 (6.49)	W10 × 22 (6.49)	W10 × 22 (6.49)	W8 × 24 (7.08)	W10 × 22 (6.49)	W8 × 24 (6.49)
30	W8 × 21 (6.16)	W8 × 21 (6.16)	W8 × 21 (6.16)	W8 × 21 (6.16)	W8 × 21 (6.16)	W8 × 21 (6.16)
31	W10 × 88 (25.9)	W16 × 57 (16.8)	W16 × 57 (16.8)	W24 × 62 (18.2)	W21 × 57 (16.7)	W24 × 62 (16.8)
32	W10 × 22 (6.49)	W10 × 22 (6.49)	W10 × 22 (6.49)	W10 × 22 (6.49)	W10 × 22 (6.49)	W10 × 22 (6.49)
33	W8 × 21 (6.16)	W8 × 21 (6.16)	W8 × 21 (6.16)	W8 × 21 (6.16)	W8 × 21 (6.16)	W8 × 21 (6.16)
34	W24 × 62 (18.2)	W16 × 57 (16.8)	W16 × 57 (16.8)	W10 × 54 (15.8)	W10 × 54 (15.8)	W10 × 54 (14.7)
35	W8 × 21 (6.16)	W8 × 21 (6.16)	W8 × 21 (6.16)	W8 × 21 (6.16)	W8 × 21 (6.16)	W8 × 21 (6.16)
36	W8 × 21 (6.16)	W8 × 21 (6.16)	W8 × 21 (6.16)	W8 × 21 (6.16)	W8 × 21 (6.16)	W8 × 21 (6.16)
37	W24 × 68 (20.1)	W24 × 68 (20.1)	W24 × 68 (20.1)	W12 × 40 (11.8)	W16 × 36 (10.6)	W12 × 40 (9.71)
38	W8 × 21 (6.16)	W8 × 21 (6.16)	W8 × 21 (6.16)	W8 × 21 (6.16)	W8 × 21 (6.16)	W8 × 21 (6.16)
39	W8 × 21 (6.16)	W8 × 21 (6.16)	W8 × 21 (6.16)	W8 × 21 (6.16)	W8 × 21 (6.16)	W8 × 21 (6.16)
40	W12 × 30 (8.79)	W12 × 30 (8.79)	W12 × 30 (8.79)	W10 × 39 (11.5)	W12 × 30 (8.79)	W10 × 39 (8.79)
41	W8 × 21 (6.16)	W8 × 21 (6.16)	W8 × 21 (6.16)	W8 × 21 (6.16)	W8 × 21 (6.16)	W8 × 21 (6.16)
42	W8 × 21 (6.16)	W8 × 21 (6.16)	W8 × 21 (6.16)	W8 × 21 (6.16)	W8 × 21 (6.16)	W8 × 21 (6.16)
43	W8 × 21 (6.16)	W8 × 21 (6.16)	W8 × 21 (6.16)	W8 × 21 (6.16)	W8 × 21 (6.16)	W8 × 21 (6.16)
44	W8 × 21 (6.16)	W8 × 21 (6.16)	W8 × 21 (6.16)	W8 × 21 (6.16)	W8 × 21 (6.16)	W8 × 21 (6.16)
45	W8 × 21 (6.16)	W8 × 21 (6.16)	W8 × 21 (6.16)	W8 × 21 (6.16)	W8 × 21 (6.16)	W8 × 21 (6.16)
46	W8 × 21 (6.16)	W8 × 21 (6.16)	W8 × 21 (6.16)	W8 × 21 (6.16)	W8 × 21 (6.16)	W8 × 21 (6.16)
47	W8 × 21 (6.16)	W8 × 21 (6.16)	W8 × 21 (6.16)	W8 × 21 (6.16)	W8 × 21 (6.16)	W8 × 21 (6.16)
48	W8 × 21 (6.16)	W8 × 21 (6.16)	W8 × 21 (6.16)	W8 × 21 (6.16)	W8 × 21 (6.16)	W8 × 21 (6.16)
49	W8 × 21 (6.16)	W8 × 21 (6.16)	W8 × 21 (6.16)	W8 × 21 (6.16)	W8 × 21 (6.16)	W8 × 21 (6.16)
50	W8 × 21 (6.16)	W8 × 21 (6.16)	W8 × 21 (6.16)	W8 × 21 (6.16)	W8 × 21 (6.16)	W8 × 21 (6.16)
51	W8 × 21 (6.16)	W8 × 21 (6.16)	W8 × 21 (6.16)	W8 × 21 (6.16)	W8 × 21 (6.16)	W8 × 21 (6.16)
52	W8 × 21 (6.16)	W8 × 21 (6.16)	W8 × 21 (6.16)	W8 × 21 (6.16)	W8 × 21 (6.16)	W8 × 21 (6.16)
53	W8 × 21 (6.16)	W8 × 21 (6.16)	W8 × 21 (6.16)	W8 × 21 (6.16)	W8 × 21 (6.16)	W8 × 21 (6.16)
54	W8 × 21 (6.16)	W8 × 21 (6.16)	W8 × 21 (6.16)	W8 × 21 (6.16)	W8 × 21 (6.16)	W8 × 21 (6.16)
55	W8 × 21 (6.16)	W8 × 21 (6.16)	W8 × 21 (6.16)	W8 × 21 (6.16)	W8 × 21 (6.16)	W8 × 21 (6.16)
56	W8 × 21 (6.16)	W8 × 21 (6.16)	W8 × 21 (6.16)	W8 × 21 (6.16)	W8 × 21 (6.16)	W8 × 21 (6.16)
57	W8 × 21 (6.16)	W8 × 21 (6.16)	W8 × 21 (6.16)	W8 × 21 (6.16)	W8 × 21 (6.16)	W8 × 21 (6.16)
58	W8 × 21 (6.16)	W8 × 21 (6.16)	W8 × 21 (6.16)	W8 × 21 (6.16)	W8 × 21 (6.16)	W8 × 21 (6.16)
Best Weight (N)	1,648,971	1,609,328	1,664,200	1,569,293	1,568,116	1,560,880
Mean Weight (N)	1,814,920	1,670,558	1,754,082	1,664,278	1,653,367	1,632,878
Std. (N)	305,365	81,012	152,368	72,377	69,093	7,680
OFEs	23,460	21,180	21,720	18,420	14,520	10,320

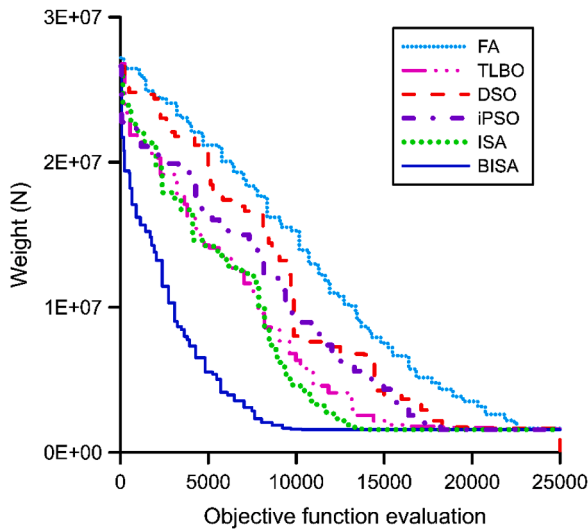


Fig. 11. The convergence history for 582-bar tower problem.

Table 17
Effect of activation period parameter (k) on the convergence rate of the algorithm

Problem	Activation period parameter (k)					
	5	10	15	20	25	30
	Iterations required to find same optimal solution					
Sphere function	110	108	111	114	118	118
72-bar truss	351	349	361	365	373	375

Algorithm (ISA). The introduced method is named as Bayesian Interactive Search Algorithm (BISA). During the optimization process, the defined Bayesian module of the proposed BISA gathers required information, and based on its activation factor (k), it is periodically engaged and tunes the algorithm’s search behavior. To acquire an optimal value for the activation factor, a sensitivity analysis is performed on this parameter and k=10 is determined as its optimum value. Subsequently, the search capability of the BISA is assessed in solving of different unconstrained mathematical functions and constrained structural problems with dynamic and static restrictions including both discrete and continuous variables. According to the acquired outcomes and registered observations, the affirmative features of the BISA method is summarized as follows.

First, the proposed BISA combines the stochastic search attribute of the metaheuristic technique with the probabilistic principles of the Bayesian approach and provides a robust search algorithm. Second, since the auxiliary Bayesian module of the proposed BISA attempts to adjust the algorithm search scheme according to the governing condition of the current problem, the proposed BISA works as a self-adaptive search technique. Third, the registered numbers of required OFEs for both constrained and unconstrained problems show that, the presented BISA, thanks to its Bayesian regulator module, decreasing the number of inefficient iterations (i.e. iteration without improvements) speeds up the convergence rate and increases the efficiency of the algorithm. To provide more insight into the convergence behavior of the proposed algorithm, this issue also is verified and shown via plotting the diversity diagrams for four distinct mathematical functions. Fourth, the attained optimal results demonstrate that the accuracy of the found optimal solutions are raised. It reveals that the supplementary Bayesian strategy regulating the search behavior of the process provides more room for the algorithm to search the problems’ domains more precisely. Fifth, the attained statistical data (i.e. the mean and standard deviation values) indicates that the proposed BISA could improve the stability of the optimization process in the cases of both mathematical and engineering problems. Consequently, comparing the reported optimal results, especially for the 72-bar, 120-bar, 200-bar, and 582-bar structural systems, points that as the complexity of the optimization problem rises, the affirmative effect of the auxiliary Bayesian strategy increases. This fact indicates that, the proposed BISA has a remarkable potential to be employed as a self-adaptive and general search technique for solving other complex optimization problems. As a future work, it is intended to apply the proposed BISA on the optimum design of the green building systems.

Authorship contributions

Please indicate the specific contributions made by each author (list the authors’ initials followed by their surnames, e.g., Y.L. Cheung). The name of each author must appear at least once in each of the three categories below.

Declaration of Competing Interest

The authors declare that they have no known competing financial interests or personal relationships that could have appeared to influence the work reported in this paper.

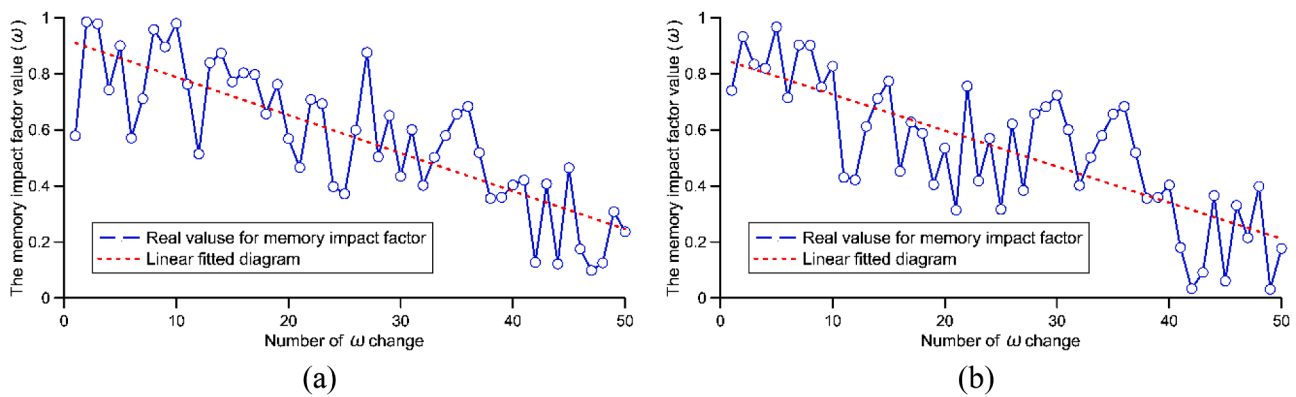


Fig. 12. Schematic for 50 different values for memory impact factor (k) for (a) sphere function and (b) the 72-bar truss structure.

Acknowledgements

All persons who have made substantial contributions to the work reported in the manuscript (e.g., technical help, writing and editing assistance, general support), but who do not meet the criteria for authorship, are named in the Acknowledgements and have given us their written permission to be named. If we have not included an Acknowledgements, then that indicates that we have not received substantial contributions from non-authors.

References

- [1] Lee KS, Geem ZW. A new meta-heuristic algorithm for continuous engineering optimization: harmony search theory and practice. *Computer Methods in Applied Mechanics and Engineering* 2005;194:3902–33.
- [2] Noel MM. A new gradient based particle swarm optimization algorithm for accurate computation of global minimum. *Applied Soft Computing* 2012;12:353–9.
- [3] Yang X-S. A New Metaheuristic Bat-Inspired Algorithm. In: González JR, Pelta DA, Cruz C, Terrazas G, Krasnogor N, editors. *Nature Inspired Cooperative Strategies for Optimization (NICSO 2010)*. Berlin, Heidelberg: Springer Berlin Heidelberg; 2010. p. 65–74.
- [4] Cheng M-Y, Prayogo D. Symbiotic Organisms Search: A new metaheuristic optimization algorithm. *Computers & Structures* 2014;139:98–112.
- [5] Gholizadeh S, Razavi N, Shojaei E. Improved black hole and multiverse algorithms for discrete sizing optimization of planar structures. *Engineering Optimization* 2019;51:1645–67.
- [6] Hasançebi O, Erbatuf F. On efficient use of simulated annealing in complex structural optimization problems. *Acta Mechanica* 2002;157:27–50.
- [7] Achtziger W, Stolpe M. Global optimization of truss topology with discrete bar areas—Part II: Implementation and numerical results. *Computational Optimization and Applications* 2007;44:315–41.
- [8] Camp CV, Bichon BJ. Design of Space Trusses Using Ant Colony Optimization. *Journal of Structural Engineering* 2004;130:741–51.
- [9] Lopez RH, Luersen MA, Cursi ES. Optimization of laminated composites considering different failure criteria. *Composites Part B: Engineering* 2009;40: 731–40.
- [10] Cheng J. Optimum design of steel truss arch bridges using a hybrid genetic algorithm. *Journal of Constructional Steel Research* 2010;66:1011–7.
- [11] Toğan V, Mortazavi A. Sizing optimization of skeletal structures using teaching-learning based optimization. *Optimization and Control: Theories Applications* 2017;7:12.
- [12] Gholizadeh S, Ebadijalal M. Performance based discrete topology optimization of steel braced frames by a new metaheuristic. *Advances in Engineering Software* 2018;123:77–92.
- [13] Moloodpoor M, Mortazavi A, Ozbalta N. Thermal analysis of parabolic trough collectors via a swarm intelligence optimizer. *Solar Energy* 2019;181:264–75.
- [14] Mortazavi A, Toğan V, Moloodpoor M. Solution of structural and mathematical optimization problems using a new hybrid swarm intelligence optimization algorithm. *Advances in Engineering Software* 2019;127:106–23.
- [15] Mortazavi A. Large-scale structural optimization using a fuzzy reinforced swarm intelligence algorithm. *Advances in Engineering Software* 2020;142:102790.
- [16] Mortazavi A. Size and layout optimization of truss structures with dynamic constraints using the interactive fuzzy search algorithm. *Engineering Optimization* 2020;1–23.
- [17] Bigham A, Gholizadeh S. Topology optimization of nonlinear single-layer domes by an improved electro-search algorithm and its performance analysis using statistical tests. *Structural and Multidisciplinary Optimization* 2020;62:1821–48.
- [18] Pourmoosavi G, Ghasemi SAM, Azar BF, Talatahari S. Shear design curves of unstiffened plate girder web panels at high temperatures. *Journal of Constructional Steel Research* 2020;164:105808.
- [19] Mortazavi A, Toğan V, Daloğlu A, Nuhoglu A. Comparison of Two Metaheuristic Algorithms on Sizing and Topology Optimization of Trusses and Mathematical Functions. *Gazi University Journal of Science* 2018;31:416–35.
- [20] Mlakar U, Fister I, Fister I. Hybrid self-adaptive cuckoo search for global optimization. *Swarm and Evolutionary Computation* 2016;29:47–72.
- [21] Ho-Huu V, Nguyen-Thoi T, Vo-Duy T, Nguyen-Trang T. An adaptive elitist differential evolution for optimization of truss structures with discrete design variables. *Computers & Structures* 2016;165:59–75.
- [22] Tang K, Li Z, Luo L, Liu B. Multi-strategy adaptive particle swarm optimization for numerical optimization. *Engineering Applications of Artificial Intelligence* 2015; 37:9–19.
- [23] Bratton D, Kennedy J. Defining a Standard for Particle Swarm Optimization. In: 2007 IEEE Swarm Intelligence Symposium; 2007. p. 120–7.
- [24] Parrott D, Xiaodong L. Locating and tracking multiple dynamic optima by a particle swarm model using speciation. *IEEE Transactions on Evolutionary Computation* 2006;10:440–58.
- [25] Mortazavi A. The Performance Comparison of Three Metaheuristic Algorithms On the Size, Layout and Topology Optimization of Truss Structures. *Mugla Journal of Science and Technology* 2019;5:28–41.
- [26] Mortazavi A, Toğan V. Triangular units based method for simultaneous optimizations of planar trusses. *Advances in Computational Design* 2017;2: 195–210.
- [27] Wen-Jun Z, Xiao-Feng X. DEPSO: hybrid particle swarm with differential evolution operator. In: SMC'03 Conference Proceedings. 2003 IEEE International Conference on Systems, Man and Cybernetics. Conference Theme - System Security and Assurance (Cat. No.03CH37483). 3814; 2003. p. 3816–21.
- [28] Deep K, Das K. Performance improvement of real coded genetic algorithm with Quadratic Approximation based hybridisation. *International Journal of Intelligent Defence Support Systems* 2009;2.
- [29] Deep K, Bansal JC. Hybridization of particle swarm optimization with quadratic approximation. *OPSEARCH* 2009;46:3–24.
- [30] Barroso ES, Parente E, Cartaxo de Melo AM. A hybrid PSO-GA algorithm for optimization of laminated composites. *Structural and Multidisciplinary Optimization* 2017;55:2111–30.
- [31] Yalaoui N, Ouazene Y, Yalaoui F, Amodeo L, Mahdi H. Fuzzy-metaheuristic methods to solve a hybrid flow shop scheduling problem with pre-assignment. *International Journal of Production Research* 2013;51:3609–24.
- [32] Nobile MS, Cazzaniga P, Besozzi D, Colombo R, Mauri G, Pasi G. Fuzzy Self-Tuning PSO: A settings-free algorithm for global optimization. *Swarm and Evolutionary Computation* 2018;39:70–85.
- [33] Xin B, Chen J, Peng Z, Pan F. An adaptive hybrid optimizer based on particle swarm and differential evolution for global optimization. *Science China Information Sciences* 2010;53:980–9.
- [34] Deng W, Chen R, He B, Liu Y, Yin L, Guo J. A novel two-stage hybrid swarm intelligence optimization algorithm and application. *Soft Computing* 2012;16: 1707–22.
- [35] Finotto VC, da Silva WRL, Valásek M, Štemberk P. Hybrid fuzzy-genetic system for optimising cabled-truss structures. *Advances in Engineering Software* 2013;62–63: 85–96.
- [36] Olivas F, Valdez F, Castillo O. Ant Colony Optimization with Parameter Adaptation Using Fuzzy Logic for TSP Problems. In: Melin P, Castillo O, Kacprzyk J, editors. *Design of Intelligent Systems Based on Fuzzy Logic, Neural Networks and Nature-Inspired Optimization*. Cham: Springer International Publishing; 2015. p. 593–603.
- [37] Mortazavi A, Toğan V. Simultaneous size, shape, and topology optimization of truss structures using integrated particle swarm optimizer. *Structural and Multidisciplinary Optimization* 2016;54:715–36.
- [38] Kumar A, Misra RK, Singh D. Improving the local search capability of Effective Butterfly Optimizer using Covariance Matrix Adapted Retreat Phase. In: 2017 IEEE Congress on Evolutionary Computation (CEC); 2017. p. 1835–42.
- [39] Lieu QX, Do DTT, Lee J. An adaptive hybrid evolutionary firefly algorithm for shape and size optimization of truss structures with frequency constraints. *Computers & Structures* 2018;195:99–112.
- [40] Mortazavi A, Toğan V, Nuhoglu A. Interactive search algorithm: A new hybrid metaheuristic optimization algorithm. *Engineering Applications of Artificial Intelligence* 2018;71:275–92.
- [41] Mortazavi A. Interactive fuzzy search algorithm: A new self-adaptive hybrid optimization algorithm. *Engineering Applications of Artificial Intelligence* 2019; 81:270–82.
- [42] Le DT, Bui D-K, Ngo TD, Nguyen Q-H, Nguyen-Xuan H. A novel hybrid method combining electromagnetism-like mechanism and firefly algorithms for constrained design optimization of discrete truss structures. *Computers & Structures* 2019;212:20–42.
- [43] Sun L, Chen S, Xu J, Tian Y. Improved Monarch Butterfly Optimization Algorithm Based on Opposition-Based Learning and Random Local Perturbation. *Complexity* 2019;2019:20.
- [44] Mortazavi A. A new fuzzy strategy for size and topology optimization of truss structures. *Applied Soft Computing* 2020;93:106412.
- [45] Kahraman HT, Aras S. Investigation of the Most Effective Meta-Heuristic Optimization Technique for Constrained Engineering Problems. Cham: Springer International Publishing; 2020. p. 484–501.
- [46] Mortazavi A. Comparative assessment of five metaheuristic methods on distinct problems. *Dicle University Journal of Engineering* 2019;10:879.
- [47] Zhou Z, Shi Y. Inertia Weight Adaptation in Particle Swarm Optimization Algorithm. In: Tan Y, Shi Y, Chai Y, Wang G, editors. *Advances in Swarm Intelligence*. Berlin, Heidelberg: Springer Berlin Heidelberg; 2011. p. 71–9.
- [48] Nickabadi A, Ebadzadeh MM, Safabakhsh R. A novel particle swarm optimization algorithm with adaptive inertia weight. *Applied Soft Computing* 2011;11:3658–70.
- [49] Qin Z, Yu F, Shi Z, Wang Y. Adaptive Inertia Weight Particle Swarm Optimization. *Artificial Intelligence and Soft Computing* 2006;40:450–9.
- [50] Bishop C. *Neural networks for pattern recognition*. Oxford: Clarendon Press; 2005.
- [51] Yang X-S. Firefly Algorithms for Multimodal Optimization. In: Watanabe O, Zeugmann T, editors. *Stochastic Algorithms: Foundations and Applications*. Berlin, Heidelberg: Springer Berlin Heidelberg; 2009. p. 169–78.
- [52] Rao RV, Savsani VJ, Vakharia DP. Teaching-learning-based optimization: A novel method for constrained mechanical design optimization problems. *Computer-Aided Design* 2011;43:303–15.

- [53] Das KN, Singh TK. Drosophila Food-Search Optimization. *Applied Mathematics and Computation* 2014;231:566–80.
- [54] Mortazavi A, Togan V, Nuhoglu A. An integrated particle swarm optimizer for optimization of truss structures with discrete variables. *Structural Engineering and Mechanics* 2017;61:359–70.
- [55] N.H. A, M.Z. A, Suganthan PN, Liang JJ, B.Y. Q. Technical Report. Zhengzhou: Nanyang Technological University, Singapore, School of Computer Information Systems, Jordan University of Science and Technology, Jordan, School of Electrical Engineering, Zhengzhou University; 2017.
- [56] Gholizadeh S, Milany A. An improved fireworks algorithm for discrete sizing optimization of steel skeletal structures. *Engineering Optimization* 2018;50: 1829–49.
- [57] Gholizadeh S, Danesh M, Gheytratmand C. A new Newton metaheuristic algorithm for discrete performance-based design optimization of steel moment frames. *Computers & Structures* 2020;234:106250.